

## Higher curvature black holes

---

**Xián O. Camanho,<sup>a</sup> José D. Edelstein,<sup>a,b</sup>**

<sup>a</sup>*Department of Particle Physics and IGFAE, University of Santiago de Compostela,  
E-15782 Santiago de Compostela, Spain*

<sup>b</sup>*Centro de Estudios Científicos,  
Valdivia, Chile*

*E-mail:* [xian.otero@rai.usc.es](mailto:xian.otero@rai.usc.es), [jose.edelstein@usc.es](mailto:jose.edelstein@usc.es)

**ABSTRACT:** We revisit the study of (A)dS black holes in Lovelock theories. We present a new tool that allows to attack this problem in full generality. In analyzing spherically symmetric Lovelock black holes with non-planar horizon topologies many novel and interesting features are observed. Among them, the existence of maximally symmetric vacua do not supporting black holes in vast regions of the space of gravitational couplings, multi-horizon black holes, and branches of solutions that suggest the existence of a rich diagram of phase transitions. The appearance of naked singularities seems unavoidable in some cases, raising the question about the fate of the cosmic censorship conjecture in these theories. There is a preferred branch of solutions for planar black holes, as well as non-planar black holes with high enough mass or temperature. Our study clarifies the role of all branches of solutions, including asymptotically dS black holes, and whether they should be considered when studying these theories in the context of AdS/CFT or not.

**KEYWORDS:** Black holes. Lovelock gravity. Higher curvature corrections. AdS/CFT.

---

## Contents

<b>1</b>	<b>Introduction</b>	<b>1</b>
<b>2</b>	<b>Lovelock gravity</b>	<b>3</b>
<b>3</b>	<b>Lovelock black holes, a novel approach</b>	<b>4</b>
3.1	Thermodynamics	12
3.2	Horizons and naked singularities	16
<b>4</b>	<b>Taxonomy of Lovelock black holes</b>	<b>18</b>
4.1	The Einstein-Hilbert branch	18
4.2	AdS (other than EH) branches	21
4.3	dS branches	23
<b>5</b>	<b>Heat capacity and local thermodynamic stability</b>	<b>26</b>
<b>6</b>	<b>Hawking-Page-like phase transitions</b>	<b>31</b>
6.1	Spherical black holes	32
6.2	Hyperbolic black holes	34
<b>7</b>	<b>Discussion</b>	<b>35</b>

---

## 1 Introduction

Lovelock gravities are the higher dimensional cousins of general relativity. If one assumes that the space-time dimensionality is larger than four, the lagrangian that embodies Einstein's paradigm *gravity equals geometry*, while providing second order Euler-Lagrange equations for the metric tensor, has been constructed by David Lovelock forty years ago [1]. The simplest Lovelock lagrangian is the well-known Gauss-Bonnet term, that embodies a non-trivial dynamics for the gravitational field in five (or higher) dimensional theories. It has been explored to a large extent, possibly due to the appealing place that five-dimensional gravity occupies since Kaluza and Klein's groundbreaking papers, and also as a consequence of its appearance in string theories at low energies [2]. Since their inception, a steady attention has been devoted to scrutinize the main properties of Lovelock theories of gravity, their vacuum structure, induced cosmologies, hamiltonian formalism, dimensional reduction, wormhole configurations and, most importantly, their black hole solutions, including their formation, stability and thermodynamics. In spite of the abundant literature on the subject, most articles deal with particular cases of the general Lovelock formalism due to the intricacy endowed by the increasing number of coupling constants: there are  $[\frac{d-3}{2}]$  dimensionful quantities (alongside the Newton and cosmological constants)

in a  $d$ -dimensional theory. For this reason, many investigations on black hole solutions of Lovelock gravities are restricted to one-parameter (zero measure) subspaces in the space of couplings. It is the aim of this article to tackle the existence and main features of Lovelock black holes for arbitrary values of the full set of gravitational couplings.

Despite its debatable phenomenological interest, Lovelock gravities provide an interesting framework from a theoretical point of view for several reasons. As higher dimensional members of Einstein's general relativity family, they allow to explore several conceptual issues of gravity in depth in a broader setup. Among these, we can include features of black holes such as their existence and uniqueness theorems, their thermodynamics, the definition of their mass and entropy, the would be entropic nature of the gravitational force, etc. As we will show in this article, Lovelock black holes challenge some classical results in general relativity demanding a better understanding of them. Lovelock theories are perfect toy models to contrast our ideas about gravity. We shall recall at this point that much efforts have been devoted in the last quarter of a century in high energy physics dealing with scenarios involving higher dimensional gravity, and it is fair to say that at present it is unclear if gravity is a truly four-dimensional interaction.

A final piece of motivation comes from the theoretical framework proposed by Juan Maldacena a decade ago [3]. The AdS/CFT correspondence establishes a holographic identification between conformal field theories and quantum gravities in higher dimensional AdS spaces. Besides its original maximally supersymmetric formulation, the correspondence seems robust enough to survive its generalization to less supersymmetric scenarios [4], and even non-supersymmetric [5], as well as non-stringy realizations [6] (see also the seminal paper [7]). In particular, even if some caution remarks should be quoted at this point, the AdS/CFT correspondence seems to apply in higher dimensions too. We know very little about non-trivial conformal field theories in higher dimensions (see [8] for a recent discussion). Still, we can formally compute 2-point and 3-point stress-energy correlation functions and use positivity of the energy to show that the central charges are constrained to certain values [9–13] (this was originally discussed in the case of four-dimensional CFTs in [14–16]). Strikingly enough, these restrictions tantamount to analogous conditions on the gravitational coupling constants due to potential superluminal states propagating at the boundary of AdS that correspond to highly energetic gravitons exploring the bulk [17].

As soon as we invoke higher dimensionality, Lovelock gravities turn out to be on an equal footing with Einstein-Hilbert theory. Applications of AdS/CFT towards the understanding of the hydrodynamics of CFT plasmas in arbitrary dimensions demands a proper understanding of Lovelock black holes in AdS. This provides the final bit of motivation to pursue the present investigation. Regardless of the phenomenological dimensionality required by these applications, it is customarily the case that pushing some ideas to their extremes, besides verifying their robustness, allows to discover novel features that are hidden in the somehow simpler original formulation (see, for instance, [18] for a beautiful recent example of this statement).

The paper is organized as follows. We give a brief introduction on the main features of Lovelock gravity in section 2. Section 3 is devoted to present our proposal to deal with generic black holes in Lovelock theory. Finding an analytic black hole solution requires to

explicitly solve a polynomial equation and we are certainly restricted by the implications of Galois theory; meaningly, quartic is the highest order polynomial equation that can be generically solved by radicals (Abel-Ruffini theorem). However, an implicit solution can be found, and we develop some tools to extract all relevant information, mainly their horizon structure and thermodynamics. We perform a detailed classification of all possible black hole solutions in section 4, including the case of asymptotically dS solutions, and all possible horizon topologies within maximally symmetric configurations. Section 5 is devoted to study the specific heat of the whole family of black holes and we discuss their local thermodynamic stability. We find that Hawking-Page-like phase transitions should generically be present, a discussion that is part of section 6. Our analysis leads to some puzzles about the cosmic censorship conjecture in Lovelock theories. We end by discussing our results and commenting on some avenues for future research in section 7.

*Note added:* While finishing the writing up of this article we became aware of related research being pursued by H. Maeda, S. Willison and S. Ray [19].

## 2 Lovelock gravity

Lovelock gravity is the most general second order gravity theory in higher-dimensional spacetimes, and it is free of ghosts when expanding about flat space [1, 20]. The action can be written in terms of differential forms<sup>1</sup> as

$$\mathcal{I} = \frac{1}{16\pi G_N (d-3)!} \sum_{k=0}^K \frac{c_k}{d-2k} \int \mathcal{R}^{(k)}, \quad (2.1)$$

$G_N$  being the Newton constant in  $d$  spacetime dimensions and where  $c_k$  is a set of couplings with length dimensions  $L^{2(k-1)}$ ,  $L$  being some length scale related to the cosmological constant.  $K$  is a positive integer,  $K \leq \lfloor \frac{d-1}{2} \rfloor$ .  $\mathcal{R}^{(k)}$  is the exterior product of  $k$  curvature 2-forms with the required number of vierbeins to construct a  $d$ -form,

$$\mathcal{R}^{(k)} = \epsilon_{f_1 \dots f_d} R^{f_1 f_2} \wedge \dots \wedge R^{f_{2k-1} f_{2k}} \wedge e^{f_{2k+1}} \wedge \dots \wedge e^{f_d}. \quad (2.2)$$

The zeroth and first term in (2.1) correspond, respectively, to the cosmological term and the Einstein-Hilbert action. These are particular cases of the Lovelock theory. It is fairly easy to see that  $c_0 = L^{-2}$  and  $c_1 = 1$  correspond to the usual normalization of these terms.<sup>2</sup>

If we consider this action in the first order formalism, we have two equations of motion, for the connection 1-form and for the vierbein. If we vary the action with respect to the connection the resulting equation is proportional to the torsion, and so we can safely set

---

<sup>1</sup>We make use of the language of tensorial forms: out of the vierbein,  $e^a$ , and spin connection,  $\omega^a_b$ , 1-forms, we construct the Riemann curvature,  $R^a_b$ , and torsion,  $T^a$ , 2-forms:

$$R^a_b = d\omega^a_b + \omega^a_c \wedge \omega^c_b = \frac{1}{2} R^a_{b\mu\nu} dx^\mu \wedge dx^\nu, \quad T^a = de^a + \omega^a_b \wedge e^b.$$

<sup>2</sup>The cosmological constant has the customary negative value  $2\Lambda = -(d-1)(d-2)/L^2$ .

it to zero as usual, allowing us to compare our results with those coming from the usual tensorial formalism based on the metric. The second equation of motion is obtained by varying the action with respect to the vierbein. It can be cast into the form

$$\epsilon_{af_1 \dots f_{d-1}} \mathcal{F}_{(1)}^{f_1 f_2} \wedge \dots \wedge \mathcal{F}_{(K)}^{f_{2K-1} f_{2K}} \wedge e^{f_{2K+1}} \wedge \dots \wedge e^{f_{d-1}} = 0 , \quad (2.3)$$

where  $\mathcal{F}_{(i)}^{ab} \equiv R^{ab} - \Lambda_i e^a \wedge e^b$ , which makes manifest that, in principle, this theory admits  $K$  constant curvature *vacuum* solutions,

$$\mathcal{F}_{(i)}^{ab} = R^{ab} - \Lambda_i e^a \wedge e^b = 0 . \quad (2.4)$$

Inserting  $R^{ab} = \Lambda e^a \wedge e^b$  in (2.3), one finds that the  $K$  different cosmological constants are the solutions of the  $K$ -th order polynomial

$$\Upsilon[\Lambda] \equiv \sum_{k=0}^K c_k \Lambda^k = c_K \prod_{i=1}^K (\Lambda - \Lambda_i) = 0 , \quad (2.5)$$

each one corresponding to a different ‘*vacuum*’. The theory will have degenerate behavior and possibly symmetry enhancement whenever two or more effective cosmological constants coincide. This happens for a certain locus of the parameter space corresponding to the coupling constants of Lovelock theory. Curiously enough, most of the studies in the context of Lovelock theory have been performed within that degenerate locus, but significantly fewer articles were devoted to the analysis of the generic case. This article aims at making the complementary effort of digging into the non-degenerate case  $\Upsilon[\Lambda] = 0$ ,  $\Upsilon'[\Lambda] \neq 0$ . We will eventually see that, among the branches of solutions of (2.5), only one would end up being physically relevant, at least for the high mass or high temperature regime<sup>3</sup>, say  $\Lambda = \Lambda_\star$ . Thus we will see that degeneracies that do not involve  $\Lambda_\star$  are harmless, our analysis being valid for the whole parameter space, except the zero measure set  $\Upsilon[\Lambda_\star] = \Upsilon'[\Lambda_\star] = 0$ .

### 3 Lovelock black holes, a novel approach

It has been shown in [22] that Lovelock theories admit asymptotical (A)dS solutions with non-trivial horizon topologies. We can consider for instance solutions with a planar or hyperbolic symmetry as a straightforward generalization of the usual spherically symmetric ansatz,

$$ds^2 = -A(t, r) dt^2 + \frac{dr^2}{B(t, r)} + \frac{r^2}{L^2} d\Sigma_{d-2, \sigma}^2 , \quad (3.1)$$

where

$$d\Sigma_{d-2, \sigma}^2 = \frac{d\rho^2}{1 - \sigma\rho^2/L^2} + \rho^2 d\Omega_{d-3}^2 , \quad (3.2)$$

---

<sup>3</sup>Both regimes are not equivalent and in principle one may have several masses corresponding to different branches in the high temperature regime. All such branches are perturbatively unstable in that limit except for the EH-branch (see below), which is the one that has infinite mass for infinite temperature [21].

is the metric of a  $(d-2)$ -dimensional manifold of negative, zero or positive constant curvature ( $\sigma = -1, 0, 1$  parameterizing the different horizon topologies), and  $d\Omega_{d-3}^2$  is the metric of the unit  $(d-3)$ -sphere.<sup>4</sup>

It has been proven in [24] that this class of black holes admit a version of Birkhoff's theorem, in such a way that in addition to the  $SO(d-1)$ ,  $E_{d-2}$  or  $SO(1, d-2)$  isometry group, these spacetimes admit an extra timelike killing vector (for  $A, B > 0$ ). This means that these solutions of the field equations are locally isometric to their corresponding static counterparts. These can be found by means of the ansatz<sup>5</sup>

$$ds^2 = -f(r) dt^2 + \frac{dr^2}{f(r)} + \frac{r^2}{L^2} d\Sigma_{d-2, \sigma}^2, \quad (3.4)$$

These black hole solutions are all three asymptotic to a maximally symmetric space. Thus, when considering the same curvature for all of them they are locally equivalent there, but globally different. They are often referred to as topological black holes for this reason.

For  $\sigma = 0$ , which is the simplest case, using the natural frame (for  $\sigma \neq 0$  the discussion is analogous),

$$e^0 = \sqrt{f(r)} dt, \quad e^1 = -\frac{1}{\sqrt{f(r)}} dr, \quad e^a = \frac{r}{L} dx^a, \quad (3.5)$$

where  $a = 2, \dots, d-1$ . The Riemann 2-form,  $R^{ab} = d\omega^{ab} + \omega^a_c \wedge \omega^{cb}$ ,

$$\begin{aligned} R^{01} &= -\frac{1}{2} f''(r) e^0 \wedge e^1, & R^{0a} &= -\frac{f'(r)}{2r} e^0 \wedge e^a, \\ R^{1a} &= -\frac{f'(r)}{2r} e^1 \wedge e^a, & R^{ab} &= -\frac{f(r)}{r^2} e^a \wedge e^b. \end{aligned} \quad (3.6)$$

For  $\sigma \neq 0$  the expression for the curvature 2-form is basically the same except for the shift  $f \rightarrow \tilde{f} = f - \sigma$ . If we insert these expressions into the equations of motion, we get<sup>6</sup>

$$\left[ \frac{d}{d \log r} + (d-1) \right] \left( \sum_{k=0}^K c_k g^k \right) = 0, \quad (3.7)$$

---

<sup>4</sup>This does not imply that the horizon is just spherical or non-compact. By analogy with the three dimensional case (see [23] for instance) we can consider quotient spaces  $\Sigma_{d-2, \sigma}/\Gamma$  where  $\Gamma$  is a discrete subgroup of the isometry group of  $\Sigma_{d-2, \sigma}$ . Thus, even in (what we shall call) the *spherical* case, we have non-spherical possibilities; for example, one may take the horizon to be a lens space. Besides, planar or hyperbolic horizons can be made compact in this way.

<sup>5</sup>There are extra solutions with different functions in the timelike and radial direction but they are just valid for degenerate values of the cosmological constant, that is [25]  $\Upsilon[\Lambda] = \Upsilon'[\Lambda] = 0$ . In that case the most general solution is

$$ds^2 = -f(r) dt^2 + \frac{dr^2}{(-\Lambda r^2)} + \frac{r^2}{L^2} d\Sigma_{d-2, \sigma}^2, \quad (3.3)$$

for any function  $f(r)$ . This allows in particular Lifshitz-like solutions  $f(r) \sim r^{2z}$  for any value of the critical exponent  $z$ .

<sup>6</sup>Recall that, for later use, we introduced  $K$  as the natural number,  $K \leq [\frac{d-1}{2}]$ , that labels the highest non-vanishing coefficient, *i.e.*,  $c_{k>K} = 0$ .

where  $g = (\sigma - f)/r^2$ . This can be readily solved as

$$\Upsilon[g] = \sum_{k=0}^K c_k g^k = \frac{\kappa}{r^{d-1}}, \quad (3.8)$$

where  $\kappa$  is an integration constant related to the mass of the spacetime. For arbitrary dimension the spherically symmetric solutions were found in [26–28] and their extension to planar and hyperbolic symmetry is given in [22, 29].

The first question one may ask is where are the singularities of these spacetimes located. The simplest way to answer that is to calculate the curvature scalar and see where it diverges. As it depends on the metric and its derivatives these divergences can be tracked back to the divergences in the first derivative of the basic function  $g$ ,

$$g' = -\frac{(d-1)\kappa}{r^d} \Upsilon'[g]^{-1}. \quad (3.9)$$

Then, the metric is regular everywhere except at  $r = 0$  and at points where  $\Upsilon'[g] = 0$ , that is whenever the branch we are looking at coincides with any other. In such case,

$$\Upsilon'[g] = \sum_{k=1}^K k c_k g^{k-1} = 0. \quad (3.10)$$

The value of  $r$  at which this happens exhibits a curvature singularity that prevents entering a region where the metric (the function  $g$ ) becomes complex. This singularity rules out from scratch the possibility of solutions composed of different branches working at different intervals of the radial variable.

It can be easily seen that the mass parameter  $\kappa$  must be positive in the planar case ( $\sigma = 0$ ) in order for the spacetime to have a well defined horizon. We can actually rewrite the precedent equation (3.8) as

$$\sum_{k=1}^K c_k g^k = \frac{\kappa}{r^{d-1}} - \frac{1}{L^2}, \quad (3.11)$$

and realize that the equation admits a vanishing  $g$  only when  $r = r_+ \equiv (\kappa L^2)^{\frac{1}{d-1}}$ . For non-planar horizons the situation is more complicated and, in principle, some of the branches admit horizonful black hole solutions even for negative values of  $\kappa$ . The physical mass of the black hole is related to  $\kappa$  (see below) and, as such, it has to match the mass of the matter contained in that region of spacetime. Thus, this  $\kappa$  will be considered in general a positive quantity, except for hyperbolic black holes<sup>7</sup> for which some comments on negative mass solutions shall be made. In [30], indeed, the formation by collapse of such black holes with negative mass has been considered.

---

<sup>7</sup>We shall see that spherical or planar black holes always exhibit a naked singularity in the case of negative mass. The only horizon that may arise for those solutions is a cosmological one. This may also be the case for negative mass asymptotically dS branches even for hyperbolic topology.

The value of  $g$  at the would be horizon,  $r = r_+$ , is in general

$$g_+ \equiv \frac{\sigma}{r_+^2} . \quad (3.12)$$

Then, we can express  $\kappa$  as a function of the radius of the black hole horizon,  $\kappa = r_+^{d-1} \Upsilon[\sigma/r_+^2]$ . The other way around, the radius of the location of the horizons are given by solutions of the previous equation for any given value of  $\kappa$ .

The mass of the space-time can actually be found through the hamiltonian formalism [31] and is positive for positive  $\kappa$

$$M = \frac{(d-2)V_{d-2}}{16\pi G_N} \kappa = \frac{(d-2)V_{d-2}}{16\pi G_N} r_+^{d-1} \Upsilon \left[ \frac{\sigma}{r_+^2} \right] . \quad (3.13)$$

where  $V_{d-2}$  is the volume of the unit  $(d-2)$ -dimensional horizon.

In another way, this can also be understood as follows. If there is actually a mass source for the gravitational equations of motion,  $\rho = M\delta^{(d-1)}(r)$ , therefore<sup>8</sup>

$$\mathcal{E}_0 \wedge e^0 = 4\pi T_0^0 \quad \Rightarrow \quad \left[ \frac{d}{d \log r} + (d-1) \right] \frac{\kappa}{r^{d-1}} \sim \rho , \quad (3.14)$$

and, as the right hand side of the equation does not depend on the Lovelock theory we are considering, the left hand side cannot either. Thus, the relation between  $\kappa$  and the mass must be the same as in Einstein-Hilbert gravity (3.13). Also, Einstein-Hilbert has a positive energy theorem and so this reasoning suggest the same thing should apply to any Lovelock theory though this has not been proven so far. This conjectured positivity would not in principle rule out the negative mass solutions mentioned before as it may happen that the *positive mass* corresponds to the difference of the mass previously defined with the extremal one [32].

Notice that (3.8) leads to  $K$  different roots for every value of the radius and thus to  $K$  different branches, each one associated to each of the cosmological constants (2.5) (some of them may be imaginary, though), in such a way that  $g_i(r \rightarrow \infty) = \Lambda_i$ . In the planar case just one branch has a horizon at  $r = r_+$  and all the rest display naked singularities. This is so since the polynomial root  $g = 0$  has multiplicity one at  $r = r_+$ . In order to have higher multiplicity it would be necessary that also  $c_1$  vanishes, but  $c_1 = 1$  in our treatment (it corresponds to the Einstein-Hilbert (EH) term). This specific branch will be referred to as the EH-branch from now on, as it is a deformation of the only branch present in the pure Einstein-Hilbert theory and is the only one that survives when turning all the extra couplings off. For instance, in Gauss-Bonnet (GB) gravity there are two branches that read ( $c_2 \equiv \lambda L^2$ )

$$g_{(\pm)} = -\frac{1}{2L^2\lambda} \left( 1 \pm \sqrt{1 - 4\lambda \left( 1 - \frac{\kappa L^2}{r^{d-1}} \right)} \right) . \quad (3.15)$$

---

<sup>8</sup>We can relate the variations of the vierbein fields  $\delta e^a \equiv \delta e_b^a e^b$  and those of the metric as

$$\delta e_b^a = \frac{1}{2} \delta g_{\mu\nu} g^{\nu\rho} e_\rho^a e_b^\mu .$$

each one associated with a different cosmological constant. It can be readily verified that the discriminant is, in this case,  $\Delta = 1 - 4\lambda$  and so we need  $\lambda \leq 1/4$  in order to have real values.  $\lambda = 1/4$  is the critical value of the GB coupling.

Only one of the solutions,  $g_{(-)}$ , goes through  $g = 0$ , and so it is the only one with a well defined horizon in the planar case, the other one displaying a naked singularity at the origin. Remarkably enough, the solution with the well defined horizon is the one *connected* to the standard Einstein-Hilbert gravity, in the sense that it reduces to it when  $\lambda \rightarrow 0$ ,

$$g_{(-)} \approx -\frac{1}{2L^2\lambda} \left( 1 - \left[ 1 - 2\lambda \left( 1 - \frac{\kappa L^2}{r^{d-1}} \right) \right] \right) = -\frac{1}{L^2} \left( 1 - \frac{\kappa L^2}{r^{d-1}} \right). \quad (3.16)$$

The  $K$  different branches of solutions of (3.8) are continuous functions of the radial coordinate, as long as the roots of a polynomial equation depend continuously on its coefficients [33] and  $r$  enters monotonically in the zeroth order coefficient  $\tilde{c}_0(r) \equiv c_0 - \kappa/r^{d-1}$ . When  $r \rightarrow \infty$  (3.8) is nothing but the equation for the cosmological constant (2.5).

The different Lovelock couplings  $c_{k>1}$  fix the shape of the polynomial  $\Upsilon[g]$ . While varying  $r$  from  $\infty$  to  $r_+$  (see Figure 1), the function  $g(r)$  is given by the implicit solution of equation (3.8) that graphically has a remarkably simple correspond: it corresponds to climb up<sup>9</sup> a given monotonic part of the curve  $\Upsilon[g]$  starting from one of its roots (tantamount of a given comological constant) until  $g$  reaches its horizon value. If we decrease  $r$  further

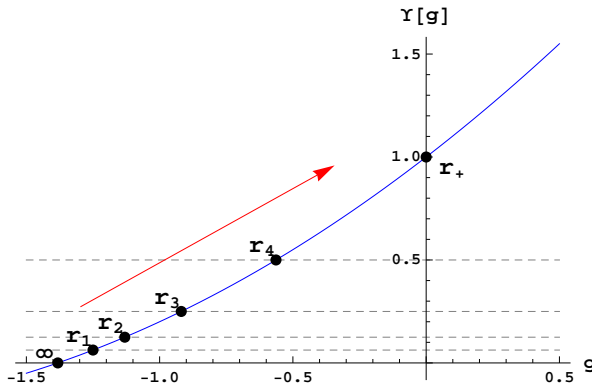


**Figure 1.** The polynomial  $\Upsilon[g]$  for the case  $K = 2$ , *i.e.*, GB theory (with  $\lambda = 0.2$  and  $L = 1$ ), in arbitrary space-time dimension, for different values of the radius ranging from  $\infty$  to  $r_+$ ,  $r_1 > r_2 > \dots > r_+$ . The projection of the depicted points give  $g(r_i)$  for the EH-branch in the planar case ( $\sigma = 0$ ).

the solution describes the interior geometry of the black hole. The metric function  $g$  is a monotonic function of  $r$  since  $\tilde{c}_0(r)$  is so and the remaining coefficients are frozen. Then each branch can be identified with a monotonic section of the polynomial  $\Upsilon[g]$ , and can easily be visualized graphically. For the EH-branch, since  $\Upsilon'[g]$  is positive at  $g = 0$ , the function  $g(r)$  is decreasing close to  $r_+$  and so it is decreasing everywhere.

<sup>9</sup>Go down for negative masses applying the same logic. The same kind of analysis can also be performed for charged solutions just by allowing the corresponding extra term in the right hand side of (3.8).

The propagator of the graviton corresponding to the vacuum  $\Lambda_i$  is proportional to  $\Upsilon'[\Lambda_i]$  in such a way that when  $\Upsilon'[\Lambda_i] < 0$  it has the opposite sign with respect to the Einstein-Hilbert case and thus the graviton becomes a ghost. This generalizes the observation first done by Boulware and Deser [26], and, because of it, we will be just considering positive slope branches. See [34] for a recent discussion on the subject. All the relevant branches correspond then to positive slope sections of the polynomial and therefore  $g$  will be considered a monotonically decreasing function of  $r$ , in the same way as in the EH-branch.

For positive  $\kappa$  the solution runs over the points with positive value for  $\Upsilon[g]$  while for negative mass it is the other way around. Either way every branch always encounters a singularity (naked or not), either as it reaches a maximum of the polynomial (minimum for negative  $\kappa$ ) or as it extends to  $r = 0$ .

For the sake of clarity and the ease of reading, let us first classify the different types of branches that one may encounter when dealing with a Lovelock theory of gravity. The appearance of a given type of branch will depend, in general, on the specific theory considered and on the values of the different coupling constants. On the one hand, we may classify the branches by their asymptotics: AdS, flat or dS branches. In the particular case we are considering, with  $c_0 = L^{-2}$ , there are no asymptotically flat branches. The sign of the cosmological constant corresponding to the EH-branch (when real) is the opposite to  $c_0$  (or, equivalently, the same as the explicit cosmological constant, as in standard Einstein-Hilbert gravity); thus, the EH-branch is asymptotically AdS. Due to the particular features and relevance of this branch, we will consider it separately.

Some of the branches (monotonic sections of the polynomial) may also be associated to complex values of  $\Lambda$ . Therefore, they do not correspond to real metrics and should be disregarded as unphysical. We will refer to these as excluded branches, and to the sector of the parameter space where the EH-branch is excluded as the *excluded region*. This region has been originally found for the cubic case in [12] (see also [13]). We will then exhaustively classify branches on (non-EH) AdS (*i.e.*, not crossing  $g = 0$ ), EH, dS and excluded branches. The latter, being unphysical, do not need further discussion. The AdS-branches must end at a maximum of the polynomial in order not to cross  $g = 0$ . The other two cases may end at a maximum or, else, continue all the way up to  $g \rightarrow \infty$ . We will then consider two subclasses of branches: those (a) continuing all the way to infinity or (b) ending at a maximum. For the AdS-branches we will also consider two subclasses: (a) positive mass and (b) negative mass.

The other parameter entering the classification will just be the topology of the horizon,  $\sigma = -1, 0, 1$ . Looking at (3.8) and (3.12), we can recast the equation for the horizon radius as

$$\Upsilon[g_+] = \frac{\kappa}{r_+^{d-1}} = \kappa \left( \sqrt{\frac{g_+}{\sigma}} \right)^{d-1}, \quad (3.17)$$

and so we see that the right hand side is just defined for negative (positive) values of  $g_+$  for  $\sigma = -1$  ( $\sigma = 1$ ), whereas for  $\sigma = 0$  it corresponds exactly to the  $g = 0$  axis, exactly as the high mass limit,  $\kappa \rightarrow \infty$ . See the table 1 below for the schematic representation of all possible cases. It is interesting to notice that monotonicity of the function  $g$  implies that

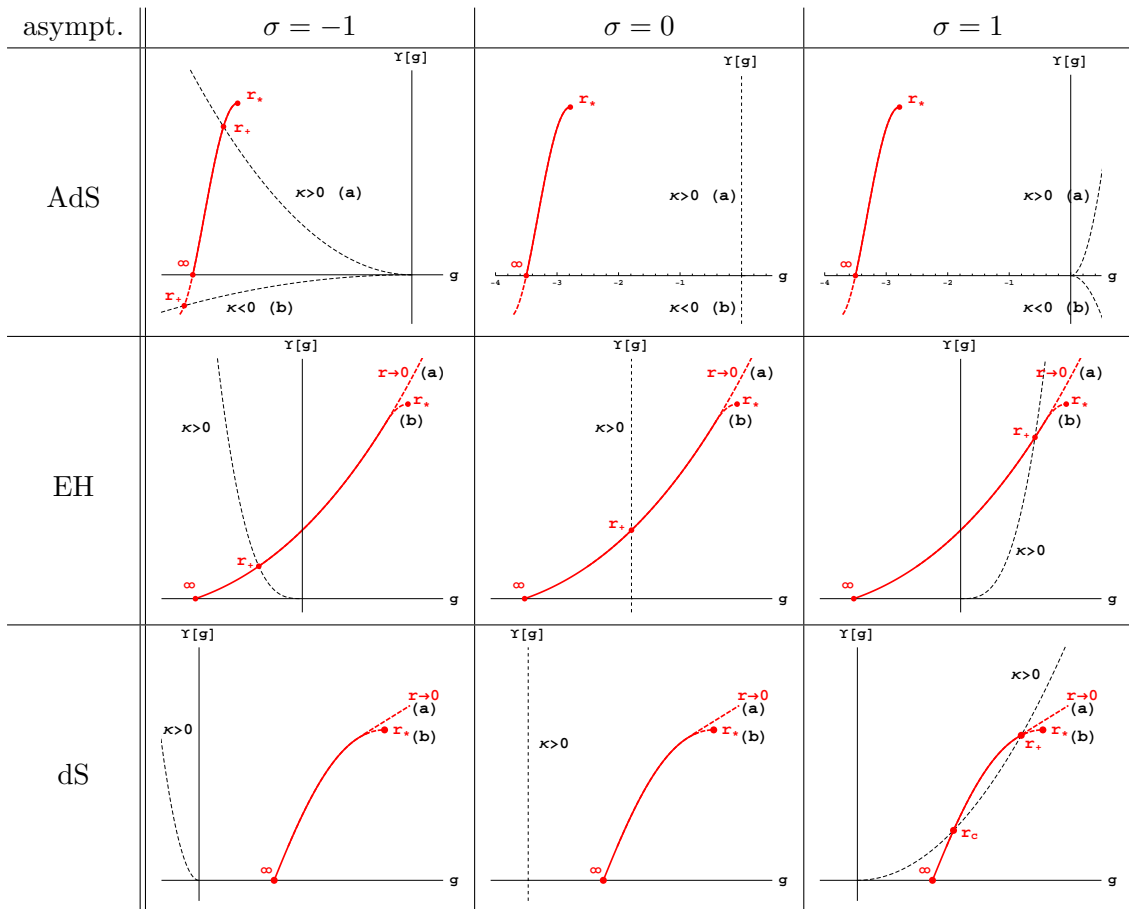


**Table 1.** Classification of (non-excluded) branches attending their asymptotics and topology.

every branch of black holes, for (positive mass) hyperbolic or planar topology, can just have one horizon. For  $\sigma = 0$  we recover just  $g_+ = 0$ , but for  $\sigma \neq 0$  we can actually have several possible values for  $g_+$  (see figure 2). Nonetheless, the right hand side of (3.17) is monotonic in  $g_+$  and each branch correspond to a monotonic part of the polynomial  $\Upsilon[g]$ . For the case of hyperbolic horizons, as the slopes of both sides have opposite signs, there can just be at most one horizon per branch.

In the positive curvature case, the determination of the number of horizons is, however, a non trivial matter. As the slope in both sides of the equation are positive we can even conceive the possibility of them crossing each other several times. In fact, this is the general case for the dS branches, that in addition to the black hole horizon have a cosmological horizon,  $r_c$  (see the bottom-right entry in table 1). Furthermore, one may also consider the existence of several black hole horizons. This is indeed the case for some regions of the parameter space with (either EH or dS) branches displaying inflection points. The simplest case where this can be observed is therefore the cubic theory, as shown in figure 2.

This very same behavior will be found in general for some region of the parameter space if the *maximally extended Lovelock theory*—that is, for  $d = 2K + 1$  or  $2K + 2$ —, as we will explain shortly. For  $d = 2K + 1$  this can be easily understood as we can always

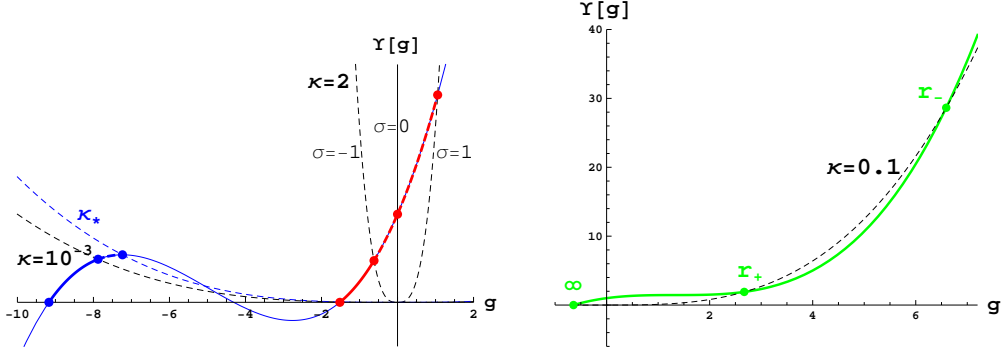


**Figure 2.** Cubic polynomial for  $L = 1$ ,  $\lambda = 1/4$  and  $\mu = 1/20$  in the first figure and  $\lambda = -0.746$  and  $\mu = 0.56$  in the second. The dashed lines are just  $\kappa(g/\sigma)^{\frac{d-1}{2}}$  for  $d = 7$  and the indicated values of  $\sigma$  and  $\kappa$  (in units of  $L$ ). The crossing of these lines with the polynomial give the possible values for  $g$  at the horizon and then of  $r_+$ . For  $\sigma = -1$  and large enough values of  $\kappa$  (or  $r_+$ ) the blue branch has a naked singularity (as it has for  $\sigma = 0, 1$ ). In the green branch we observe the occurrence of two (outer and inner, respectively) horizons,  $r_+$  and  $r_-$ . For  $d = 8$  we find a similar behavior with one further inner horizon, three in total.

construct a polynomial

$$\Upsilon[g] = \prod_{i=1}^{L \leq K} \left(1 - \frac{g}{g_i}\right) + \alpha g^K, \quad (3.18)$$

for large enough  $\alpha$  and suitable coefficients,  $g_i > \Lambda_*$ , in order to make the slope everywhere positive for the EH or dS branch with cosmological constant  $\Lambda_*$ . Then, for  $\kappa = \alpha$ , the polynomial equation has all  $g_i$  as solutions. Different (positive)  $g_i$  correspond to different spherical horizons, each degenerate  $g_i$  giving rise to a degenerate horizon. From this value, varying the mass of the solution the number of horizons will in general change. For the EH-branch, the number of black hole horizons has to be always one for high enough mass, and it is so as well in the low mass regime for  $d > 2K + 1$  as well for the EH as for any dS branch. Thus, we have in general couples of horizons appearing and disappearing depending on the values of the mass. We will always refer as  $r_+$  to the outermost horizon of the black hole, *i.e.*, the biggest root of (3.17) besides the cosmological horizon, if present. The very same logic applies to the case of negative mass black holes with hyperbolic horizon. We will comment more on this later on.

The *physical* or untrapped region of the spacetime ( $f > 0$ ) is that located to the left of the dashed line in all figures appearing in table 1. The region to the right corresponds to the inside of the would be horizon or trapped region ( $f < 0$ ). We will also have more untrapped regions inside the black hole in the presence of several black hole horizons.

The only missing piece are the excluded branches. In this case the monotonic part of the polynomial ends (towards the left) at a minimum without ever touching the  $g$ -axis (see figure 3). Thus, these spacetimes have two singularities, one for small values of the radial coordinate at the maximum, and another one for large values of  $r$  at the minimum. In the cases where we can just have one horizon, the nakedness of the singularity associated with

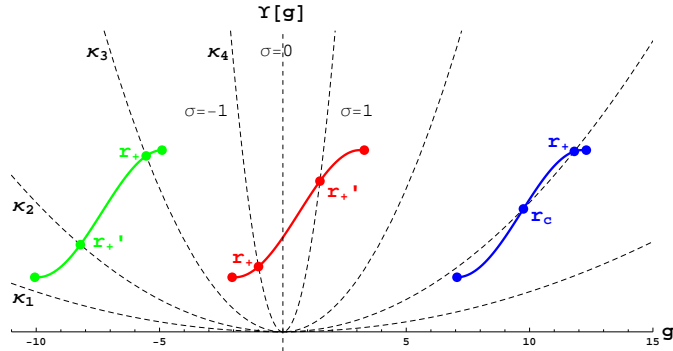


**Figure 3.** Three examples of excluded branches running over negative, negative and positive, and just negative values of  $g$  respectively. We also plot the values of the horizons for several values of the mass  $\kappa_1 < \kappa_2 < \kappa_3 < \kappa_4$  and all the topologies. The one crossing  $g = 0$  corresponds to the (excluded) EH-branch. When the EH-branch is excluded we say that we are in the excluded region of the parameter space. The blue branch describes a well defined spacetime for some values of the mass with both singularities hidden behind the black hole and the cosmological horizon. The same may happen for a excluded EH-branch in the presence of one or more inflection points.

the minimum cannot be avoided. In the  $\sigma = 1$  case we may have two (or more) horizons, each of them hiding a singularity and describing a regular spacetime in between.

We observe that, contrary to what happens for planar topology, there exists the possibility of having several branches with a horizon for  $\sigma \neq 0$ . Some of them may be discarded by means of Boulware-Deser-like instabilities, while some other branches will appear or disappear depending on the actual values of the different couplings and  $\kappa$ . These coefficients fix the shape of the polynomial and, as they vary, some branches can become pathological either in reason of their cosmological constant becoming imaginary or because of the disappearance of the would be event horizon behind a naked singularity.

The existence of at least one horizon fixes hyperbolic topology as the only possible one for AdS branches (see the first row in table 1), as well as it sets an upper bound on the mass of such spacetimes (corresponding to  $r_*$  in such plot). It also sets a lower bound if we consider the possibility of negative mass black holes in those branches. Also this sets a lower bound for the spherical black hole in the EH-branch of type (b) (or even (a) in the maximal case,  $d = 2K + 1$ ). For dS branches this requirement also fixes the only possible topology as spherical at the same time as it imposes a double bound, upper and lower, as will be discussed further later on.

### 3.1 Thermodynamics

The EH-branch is the only one that does not become pathological (at least for  $\sigma = 0$  or  $-1$ ). It is actually the branch that reduces to the usual Einstein-Hilbert solution when turning off all the extra couplings; it is the only one with a well defined limit in that case. For  $\sigma = 1$ , the horizon disappears if there is a maximum of the polynomial for a positive  $g_*$ , and the value  $g_+$  at the (would be) horizon is greater than the value at the maximum,  $g_+ > g_*$ . Then, given that two roots coincide at  $g_*$ , a curvature singularity arises which is

not hidden behind the horizon. This can be prevented by considering a big enough black hole. In that way we also ensure the stability of the black hole, as it happens for the usual Einstein-Hilbert AdS-Schwarzschild black hole. For large  $r_+$ , we can approximate

$$M \sim T^{d-1}, \quad (3.19)$$

which coincides with the planar case. Then,  $dM/dT > 0$  and the black hole is locally thermodynamically stable; it can be put in equilibrium with a thermal bath. In general, this will not happen for small black holes. This points towards the occurrence of Hawking-Page-like phase transitions of the kind interpreted as confinement-deconfinement phase transitions in the corresponding dual conformal plasma [35, 36]. This has already been studied in the case of Gauss-Bonnet gravity [37, 38]. In order to further investigate this in the case of general Lovelock theories it would be necessary to calculate the free energy (the euclideanized on-shell action) associated with the black hole. This has to be studied in the non-planar case, otherwise scale invariance would only allow for phase transitions at zero temperature. The complicated structure of phase transitions would then be hidden and any black hole would represent just the stable highest temperature deconfined phase.

The other way around, if we want to consider CFTs on flat spacetime, we just need to consider flat horizon black holes, thus, just the EH-branch (see table 1), as discussed in [12]. We can further determine the asymptotic behavior of  $g$  at infinity,  $g \approx \Lambda (1 - \tilde{\kappa}/r^{d-1})$ . If we plug this expression in (3.8), we get

$$\tilde{\kappa} = -\frac{\kappa}{\Lambda \Upsilon'[\Lambda]}, \quad (3.20)$$

and, as long as the polynomial factor is positive and the cosmological constant negative,  $\tilde{\kappa}$  is positive. The well-behaved black hole associated with the EH-branch always behaves asymptotically as the usual (positive mass) AdS black hole from Einstein-Hilbert gravity. The addition of higher curvature corrections does not change the qualitative behavior of the solution in any meaningful way. These black holes have a well defined temperature

$$T = \frac{f'(r_+)}{4\pi} = \frac{r_+}{4\pi} \left[ (d-1) \frac{\Upsilon[g_+]}{\Upsilon'[g_+]} - 2g_+ \right]. \quad (3.21)$$

From this expression it is not clear what the sign of the temperature is. The sign of  $\Upsilon[g_+]$  is the same of  $\kappa$ , and then it is positive for positive mass. Then, for positive slope branches the first term is always positive for positive mass. The sign of the second term depends on  $\sigma$  in such a way that it is only negative for spherical topology ( $\sigma = 1$ ). Then the temperature is trivially positive for positive mass black holes with hyperbolic or planar topology. It is also positive for negative mass AdS black holes as will be explained shortly. This simply derives from the fact that the temperature can just change sign if at some intermediate  $r_+$  value the temperature actually vanishes, that is, if the black hole is extremal and the event horizon degenerate ( $f' = 0$ ). This very same logic will ensure the positivity of the temperature of the black hole horizon for spherical black holes. This will be explained later by using a different approach.

We will have negative temperature horizons but this is a common feature also of Einstein-Hilbert gravity. For instance, the temperature of the cosmological horizon of pure

dS space is negative in our conventions, as it is negative for the inner horizon of a Reissner-Nordstrom black hole, regardless of the asymptotics of the solution. The same will happen here.

One important feature that will be relevant later on, when discussing classical stability, is that the temperature is proportional to the derivative of the mass (3.13) with respect to the radius of the black hole horizon,

$$\frac{dM}{dr_+} = \frac{(d-2)V_{d-2}}{4G_N} r_+^{d-3} \Upsilon' [g_+] T . \quad (3.22)$$

The proportionality factor is exactly the radial derivative of the black hole entropy

$$\frac{dS}{dr_+} = \frac{1}{T} \frac{dM}{dr_+} = \frac{(d-2)V_{d-2}}{4G_N} r_+^{d-3} \Upsilon' [g_+] . \quad (3.23)$$

We can see that, as long as we are in a branch free from Boulware-Deser instabilities, the radial derivative of the mass and the entropy are positive for  $T > 0$ . On the one hand, this will be important when discussing classical instability as the heat capacity of the black hole reads

$$C = \frac{dM}{dT} = \frac{dM}{dr_+} \frac{dr_+}{dT} , \quad (3.24)$$

and then the only factor that can be negative leading to an instability is  $dT/dr_+$ . On the other hand, if we set the ground state ( $r_+ = 0$ ) entropy to vanish, the positivity of (3.23) implies the positivity of the entropy. Negative values for the entropy may however be encountered [39–43] in the case of hyperbolic horizons in which such *ground state* does not exist.<sup>10</sup> It is actually unclear what is the suitable vacuum solution to be used as a *reference state* [44].

The expression for the entropy can be easily obtained by integrating (3.23). It is the only magnitude seen so far that cannot be readily expressed in terms of the polynomial  $\Upsilon[g]$  and we need to write the sum explicitly. The result is

$$S \equiv \frac{V_{d-2}}{4G_N} r_+^{d-2} \sum_{k=1}^K k c_k \frac{d-2}{d-2k} g_+^{k-1} = \frac{A}{4G_N} \left( 1 + \sum_{k=2}^K k c_k \frac{d-2}{d-2k} g_+^{k-1} \right) , \quad (3.25)$$

and coincides with the entropy obtained by other means like the Wald entropy [45] or the euclideanized on-shell action [39]. Interestingly enough, it has been recently suggested that this expression can be extended towards the interior of the geometry by performing a radial foliation and replacing  $g_+$  by  $g(r)$ ; the resulting function,  $S(r)$  being interpreted as the information contained inside a given region of the spacetime [18]. We have fixed the integration constant such that the entropy vanishes when the horizon radius goes to zero. For planar horizons ( $g_+ = 0$ ) this formula reproduces the proportionality of entropy and area,  $A = V_{d-2} r_+^{d-2}$ , of the black hole horizon whereas it gets corrections for other topologies.

---

<sup>10</sup>Also for type (b) spherical solutions.

From these quantities we can now compute any other thermodynamic potential as the Helmholtz free energy  $F = M - TS$ ,

$$F = \frac{(d-2)V_{d-2}}{16\pi G_N} \frac{r_+^{d-1}}{\Upsilon'[g_+]} \sum_{k,m=0}^K \frac{2m-2k+1}{d-2k} k c_k c_m g_+^{k+m-1}. \quad (3.26)$$

This magnitude is relevant for processes at constant temperature to analyze the global stability of the solutions. The above expression has degree  $2K - 1$  in the numerator. Thus, that is the maximal number of zeros (for the non-planar case where  $g_+ \neq 0$ ) that may eventually correspond to Hawking-Page-like phase transitions, provided they have the adequate sign for each topology (see [46] for a concrete example in the Gauss-Bonnet theory). This expression also diverges at a maximum of the polynomial. We will comment further about this below.

Another useful application of (3.22) is to determine the sign of the temperature, which is the same as that of the variation of the mass with respect to the horizon radius. One can easily realize (see figure 4) that the sign of the temperature depends just on the direction of the change of sign of the function  $f$  across the horizon. If this sign changes from  $f < 0$

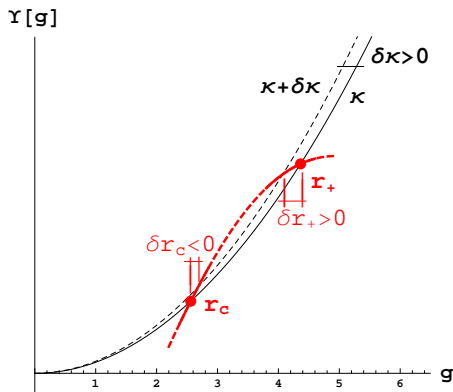


**Figure 4.** Determination of the sign of the temperature for the cosmological and black hole horizon of a dS branch. The cosmological horizon has  $T_c \propto d\kappa/dr_c < 0$  whereas the event horizon of the black hole has  $T_+ \propto d\kappa/dr_+ > 0$ . Recall that  $\text{sign}(\delta g_+) = -\text{sign}(\delta r_+)$  and the same holds for every horizon.

to  $f > 0$  as, for instance, in the cosmological horizon of any asymptotically dS spacetime, the temperature is negative, whereas it is positive in the opposite case. The black hole horizon, as the largest root of (3.17), always corresponds to the latter case, separating an untrapped region ( $f > 0$ ) from a trapped one ( $f < 0$ ), and as such it always has positive temperature. The inner horizons have alternating signs for the temperature starting from a negative one. Degenerate horizons obviously have zero temperature corresponding to extremal black holes.

### 3.2 Horizons and naked singularities

Let us start this subsection by discussing the horizon structure of the vacuum solutions. The general form of the metric function  $f$  is in this case

$$f(r) = \sigma - \Lambda r^2, \quad (3.27)$$

so it can vanish at  $r = \sqrt{\sigma/\Lambda}$ , whenever  $\sigma$  and  $\Lambda$  have the same sign, thus for hyperbolic AdS and spherical dS spacetimes. These horizons are observer dependent features since these spacetimes are maximally symmetric and, thus, any point can be considered as the origin. The dS case is widely known [47], this being the cosmological event horizon: the maximal comoving distance light can travel due to the spacetime expansion.

The AdS case is, however, more obscure as long as the horizon is actually encircling a finite size region in a similar way as a regular black hole horizon. When we consider positive mass solutions the black hole horizon is actually just a deformation of this ‘vacuum’ horizon. This has a difficult interpretation and has led to the proposal that the true ground state for hyperbolic spacetimes is not the massless one but an extremal negative mass solution [48, 49]. The cosmological horizon of pure dS spacetime has negative temperature, as discussed earlier, while for the AdS case the temperature is positive as for a regular black hole horizon.

In order to analyze the structure of horizons, let us focus on the asymptotically AdS, dS and flat black holes in Einstein-Hilbert gravity with cosmological constant (respectively,  $c_0 = L^{-2}$ ,  $-L^{-2}$  and 0) [49]. We include this simple case here for completeness and as an illustration of our method. As clearly depicted in figure 5, the only case accepting all three distinct topologies without exhibiting naked singularities is the asymptotically AdS configuration, the other two cases being well-defined just for spherical topology.<sup>11</sup> This AdS case, furthermore, has just one horizon for all three topologies. The asymptotically flat black hole has as well just one horizon corresponding to the black hole, while the asymptotically dS black hole has in general two horizons: One of them is just the deformation of the cosmological horizon already present in the maximally symmetric solution, while the other corresponds to the black hole. As the mass increases both horizons get closer to each other until, for some critical value of the mass, the so-called *Nariai mass*,

$$\kappa_{\text{Nariai}} = \frac{2L^{d-3}}{d-1} \left( \frac{d-3}{d-1} \right)^{\frac{d-3}{2}}, \quad (3.28)$$

they actually meet (they disappear for masses above that value). The untrapped region, the spacetime as we usually consider it, is comprised between the two horizons and so for this extremal case it seems to disappear. A proper limiting procedure [50] shows that the geometry remains perfectly regular as  $\kappa \rightarrow \kappa_{\text{Nariai}}$ , and becomes the geometry of the Nariai solution. This space is the direct product of a  $dS_2$  and a  $S^{d-2}$ , both with the same radius. Above this critical mass the spacetime describes again a *big crunch* spacetime.

---

<sup>11</sup>They describe a *big crunch* in the other cases. The metric function  $f$  is negative for all values of the radial variable, *i.e.*, the whole spacetime is in the trapped region with a spacelike singularity in its future.

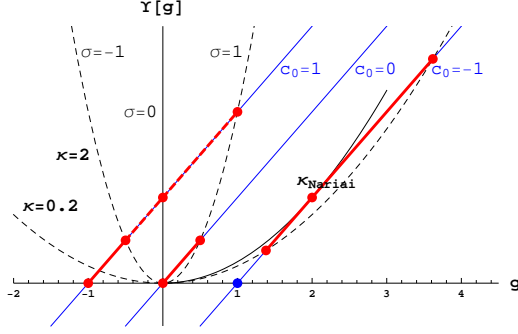


**Figure 5.** Linear polynomial corresponding to the usual EH-branch for negative ( $c_0 = 1$ ), zero ( $c_0 = 0$ ) and positive ( $c_0 = -1$ ) cosmological constants. We set  $L = 1$  for simplicity. The dashed lines are just  $\kappa (g/\sigma)^{\frac{d-1}{2}}$  for  $d = 5$ , and the indicated values of  $\sigma$  and  $\kappa$  (on units of  $L$ ). The solid black line corresponds to the critical value of the mass,  $\kappa_{\text{Nariai}} = 1/4$ , for dS black holes with spherical horizon. The crossing of these lines with the polynomial gives the possible values for  $g$  at the horizon and then of  $r_+$  (and  $r_c$ ). For  $\sigma = 1$  and  $\kappa > \kappa_{\text{Nariai}}$  (or  $r_+ > r_{\text{Nariai}}$ ), the asymptotically dS branch describes a big crunch spacetime ( $f < 0, \forall r$ ) without horizons.

In the asymptotically AdS case, a negative mass extremal hyperbolic black hole has been proposed as the ground state in Einstein-Hilbert gravity. The same would apply to any Lovelock theory. Black holes with larger (but negative) mass than this extremal one,

$$\kappa_0 = -\kappa_{\text{Nariai}} = -\frac{2L^{d-3}}{d-1} \left( \frac{d-3}{d-1} \right)^{\frac{d-3}{d-1}}, \quad (3.29)$$

have two horizons, in a way reminiscent of the asymptotically dS spherical black hole with positive mass. The difference being that in the asymptotically dS case the two correspond respectively to the cosmological and black hole horizons, while in the AdS case they are an outer and an inner horizon of the black hole (see figure 6). All horizons have positive

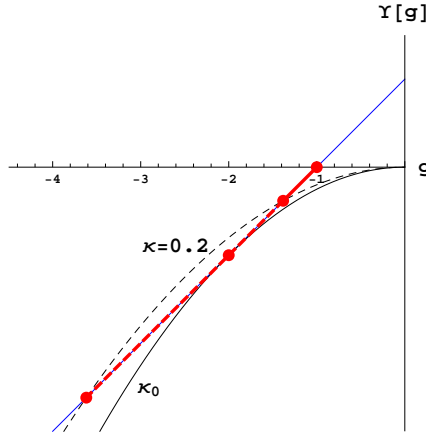


**Figure 6.** Negative mass hyperbolic black holes in Einstein-Hilbert gravity. The dashed line corresponds to a black hole with an outer and inner horizon (segment in red), while the solid line represents the extremal case,  $\kappa_0 = -\kappa_{\text{Nariai}}$ .

temperature except for the cosmological horizon. It is worth noticing that for negative

masses we are exploring a completely different section of the polynomial than for positive masses, the similarities being just due to the extremely simple form of the polynomial in the case under current analysis. In general, positive and negative mass black holes may have dramatically different features.

As we can easily see in this simple example, the existence of just one black hole horizon in all positive mass cases implies that the singularity at the origin is always spacelike, while it is timelike in the negative mass hyperbolic case due to the presence of two black hole horizons that become degenerate in the extremal limit.

## 4 Taxonomy of Lovelock black holes

We will try to describe this structure in the general Lovelock gravity<sup>12</sup> in a case by case basis, considering the previously introduced classes of black hole branches (see table 1). For the generic situation in higher dimensional Lovelock theories, some of these features will be shared and others not. Let us have a look on the many different cases that we can encounter.

### 4.1 The Einstein-Hilbert branch

The Einstein-Hilbert branch is just a deformation of the Schwarzschild-AdS black hole ( $c_0 = L^{-2}$ ) and can be identified as the branch crossing  $g = 0$  with slope  $\Upsilon'[0] = 1$ , exactly as in the Einstein-Hilbert case, and so the slope will be positive for the whole branch. This condition protects this branch from Boulware-Deser-like instabilities. When real, the cosmological constant associated with this branch is negative and so the spacetime is asymptotically AdS.<sup>13</sup> We include the relevant part of table 1 below, for the reader convenience.

Even though the EH-branch is just a deformation of the usual Schwarzschild-AdS black hole, it can be a quite dramatic one. For instance, it may happen that the polynomial has a minimum<sup>14</sup> at  $g_{\min} < 0$ , such that  $\Upsilon[g_{\min}] > 0$ , and so the Einstein-Hilbert branch has a naked singularity there (for large radius; the solution does not approach AdS asymptotically). This case was first discussed in [12, 13] for third order Lovelock theory and planar topology, but the same applies in the general case for a vast region of the space of parameters that will be named, following the aforementioned reference, the *excluded region*. In order to avoid the excluded region the value of  $\Upsilon[g_{\min}]$  at the biggest negative minimum,  $g_{\min}$ , has to be negative. The sector of the parameter space where this new kind of singularity appears has to be excluded in general, not only because of its nakedness but in reason of the perturbative instability of the corresponding solution [21]. For hyperbolic or planar topology, as this branch always crosses the  $g = 0$  point with positive slope  $\Upsilon'[0] = 1$ , it has always a horizon (just one as in the Einstein-Hilbert case) hiding the singularity of

<sup>12</sup>Some work in this direction has already been done considering just the Gauss-Bonnet case [51, 52].

<sup>13</sup>We can proceed with this analysis in an analogous way for asymptotically dS spaces, just by changing the sign of the explicit cosmological constant in the action  $c_0 \rightarrow -\frac{1}{L^2}$ , or for asymptotically flat ones, just by setting  $c_0 = 0$ .

<sup>14</sup>If there are several negative minima,  $g_{\min}$  refers to the lowest one, in absolute value.

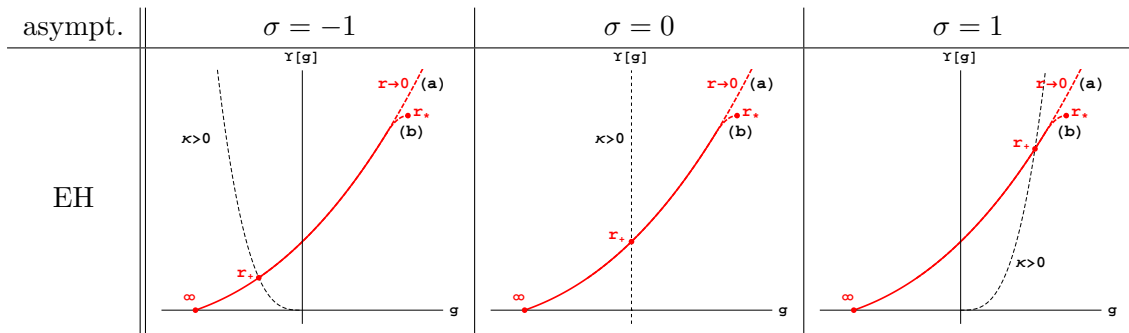


**Table 2.** Taxonomy of the EH-branch.

the geometry that has to be always located in positive values of  $g$ , either at  $g = \infty$  ( $r = 0$ ) or, else, at the value corresponding to some maximum of  $\Upsilon[g]$ , for the (b) type solution (see table 2). For hyperbolic horizons we have again the possibility of considering negative mass black holes, for masses above a certain critical value corresponding to an extremal black hole. As this case has no difference with respect to the same situation taking place in an AdS branch this will be discussed at length in the corresponding section.

The spherical case is quite more involved. For high enough mass, coinciding with the planar limit, the existence of the horizon is ensured, but this is not the case in general. For the (a) type EH-branch the existence of the horizon can be elucidated by analyzing (3.17) in the limit of small mass  $g_+ \rightarrow \infty$ . For the horizon to exist in this limit, we need the right hand side of the equation to be bigger than the left hand side. This is ensured for  $d > 2K + 1$  as in this case the biggest power in the left hand side would be smaller than  $(d - 1)/2$ . The existence of a horizon in the small mass limit ensures the existence of (at least) one for all values of the mass, simply due to the continuity of  $\Upsilon[g]$ .

The case  $d = 2K + 1$  is critical and there will be a minimal mass ( $\kappa_{\text{crit}} \leq c_K$ ) below which no horizon exists, thus a naked singularity would appear. In principle, for high enough orders of the Lovelock polynomial, more than one horizon can exist but for the critical  $d = 2K + 1$  case, at some point, all of them disappear. The number of black hole horizons determines the type of singularity situated at  $r = 0$ , space or timelike, and viceversa. For  $d > 2K + 1$  we will always have an odd number of horizons (taking into account possible degeneracies), since the singularity is in the trapped region of the spacetime. For  $d = 2K + 1$  the number of horizons depends on the value of the mass. For masses above  $c_K$  the number is odd and at least one horizon will always exist, whereas for masses below this critical mass the number of horizons will change to an even quantity, and will actually disappear at some point. Thus, the singularity is spacelike for  $d > 2K + 1$  and  $d = 2K + 1$  for masses above  $c_K$ , timelike for masses below this value in the latter case, and naked for masses below the critical value  $\kappa_{\text{crit}}$ .

The case where the EH-branch ends up at a maximum for some positive value of  $g = g_*$  ( $r = r_*$ ), or (b) type branch, is even simpler (see table 2). For some critical value of the mass the horizon radius and the singularity radius are the same,  $r_+ = r_*$ , and below that mass a naked singularity appears. This is very similar to the situation described in the previous paragraph for  $d = 2K + 1$ , the only difference being that in that case the radius

of the singularity is zero,  $r_* = 0$ .

The simplest example of Lovelock theory is GB gravity, where we have just two branches, one of them suffering from BD instabilities. The remaining branch is thus an EH-branch. For  $\lambda > 0$  this branch is of the (a) type, extending all the way up to a singularity situated at  $r = 0$ . For  $\lambda < 0$ , instead, this branch has a maximum at positive values of  $g$  (see figure 7). This is a singularity at a finite value of  $r$  that may or may not be naked

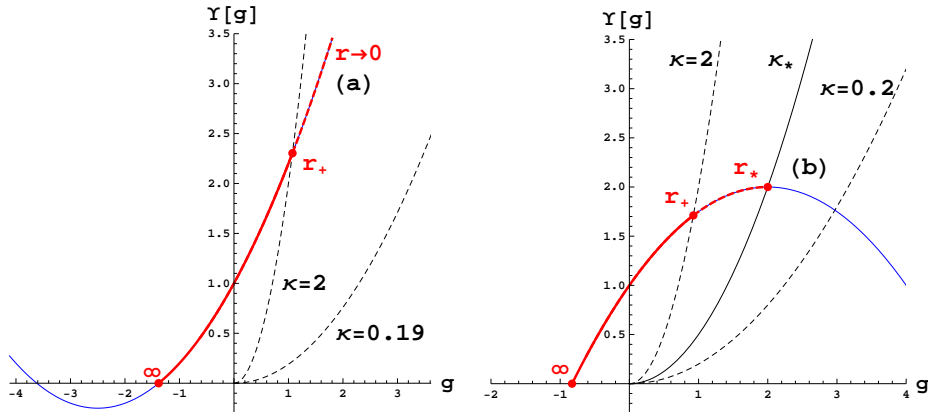


**Figure 7.** EH-branch in GB gravity in 5 dimensions for  $\lambda = 1/5$  and  $\lambda = -1/4$  respectively (we set  $L = 1$  for simplicity). The dashed curves correspond to the  $\kappa (g_+/\sigma)^{\frac{d-1}{2}}$  for the quoted values of  $\kappa$  and spherical topology ( $\sigma = 1$ ). The singularity becomes naked for  $\kappa \leq \lambda = 0.2$  in the first case and for  $\kappa \leq \kappa_* = 0.5$  in the second case. For higher dimensions the second figure would be qualitatively the same with just a different value of the critical mass. The first one, instead, changes as long as the horizon exists for all positive values of  $\kappa$  in that case. For the (b) type branches the singularity is always located at  $r_* = \sqrt{-2\lambda} L$ .

depending on the value of the mass. The mass for which the horizon coincides with the singularity is

$$\kappa_* = \frac{1}{2}(1 - 4\lambda)(-2\lambda L^2)^{\frac{d-3}{2}}. \quad (4.1)$$

For bigger masses we have a well defined horizon while below this bound the singularity becomes naked.

Another intriguing possibility, that cannot be observed within the simple setting of GB gravity, is the would be appearance of several black hole horizons. For this to happen we need inflection points in  $\Upsilon[g]$ , and so the minimal example would be the cubic Lovelock theory. In the critical  $d = 7$  case, we have the possibility of obtaining two black hole horizons for some regions of the space of parameters, while this number is three in higher dimensions. One remarkable thing worth noticing here is that, as couples of horizons appear or disappear when we vary the value of the mass, the value of  $r_+$  may change discontinuously, given that it is defined as the biggest of the black hole horizons. Thus, the temperature, as a function of the mass of the black hole, also varies discontinuously when crossing the value of the mass for which the outermost couple of horizons appear or disappear, one of the sides of the discontinuity has zero temperature (since the black

hole is extremal for such critical mass) while the other has finite temperature.<sup>15</sup> We may interpret these extremal states as black hole ground states, each one for a given range of values for the mass. These seem naively accessible by evaporation and, thus, point towards a violation of the third law of black hole dynamics, as pointed out in [57]. They are in general unstable solutions [58, 59], though. At low temperatures, this particular branch will have several possible black hole masses and transitions might occur among them and the thermal vacuum. As for temperatures close to zero the free energy essentially coincides with the mass, the globally preferred solution is the less massive one and thus the vacuum. We will comment more on this later on.

## 4.2 AdS (other than EH) branches

The second class of branches that we describe in what follows are asymptotically AdS black holes different from the EH-branch. The latter will just be included for the discussion of negative mass solutions as the analysis will be exactly the same for it in that case.

Consider first the positive mass solutions. This so called AdS branches always end at a maximum of the polynomial then. As already discussed before the existence of a horizon

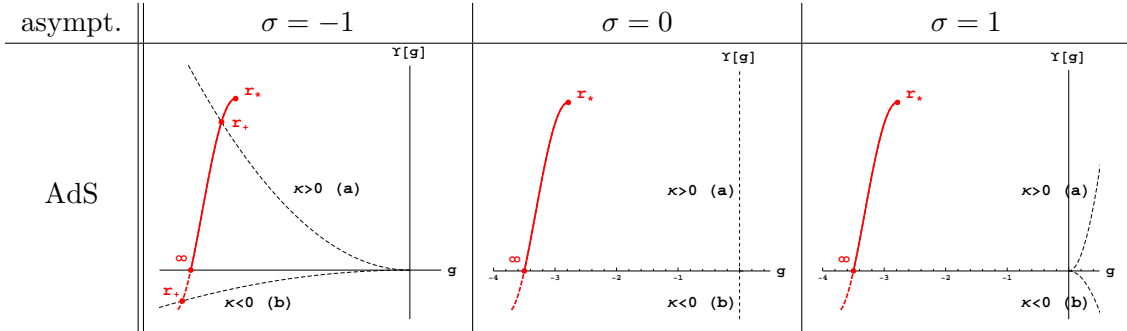


**Table 3.** Taxonomy of the AdS (other than EH) branches.

hiding the singularity fixes the only possible topology for such branches. As the considered sections of the polynomial run just over negative values of  $g$  horizons exist just for  $\sigma = -1$ . On the other cases the solutions describe a spacetime with a timelike naked singularity. This black holes will in general have one horizon in exactly the same way as the EH-branch counterparts. However, the condition for the existence of a horizon sets an upper bound on the mass,  $\kappa < \kappa_{max}$ , where  $\kappa_{max}$  corresponds to the critical value of  $\kappa$  for which the radius of the horizon coincide with that of the singularity,  $r_+ = r_{max}$ , i. e.

$$\kappa_{max} = r_{max}^{d-1} \Upsilon[g_{max}] . \quad (4.2)$$

In Einstein-Hilbert gravity when we encounter a naked singularity with positive mass is always in the case of multi-horizon black holes as while varying the parameters of the solution two horizons merge and disappear leaving the singularity naked. We pass by an

<sup>15</sup>In general inner horizons are considered unstable [53–56] and perhaps we cannot trust our solution behind that horizon, but we still have this discontinuity as we throw something across the horizon of the small black hole.

extremal solution before getting the naked singularity. The case we are describing here is somehow different as the black horizon is just one and cannot degenerate as we increase the mass approaching the critical value. Then the solution infinitesimally close to the critical one has non-zero temperature, diverging as we approach the bound. In that way this limit is more similar to the low mass limit of Schwarzschild black holes than to the usual naked singularities in Einstein-Hilbert gravity. The difference is that whereas for Schwarzschild black holes the limit leads to a regular spacetime (vacuum spacetime in fact) in this case such spacetime has a naked singularity.

For negative mass solutions the analysis of the existence of black holes and its number is quite more complicated. The main qualitative feature that may differ from the usual Einstein-Hilbert case is the possibility of having a minimum of the polynomial associated to the branch under analysis (see blue and red branches in figure 8 for instance). We will

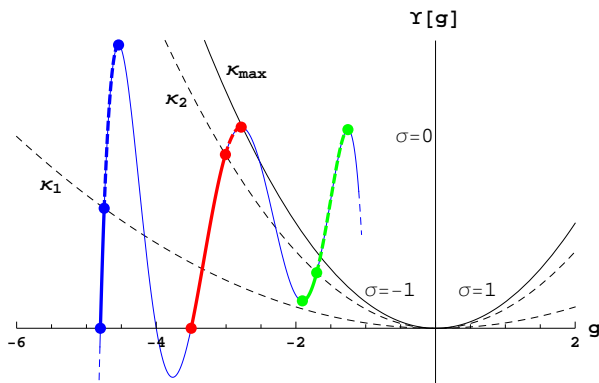


**Figure 8.** Qualitative representation of (positive mass) AdS branches of different types. The blue and the red branches will be referred to as type (b1) and (b2) respectively when considered for negative masses, and the green one is an excluded branch. There are asymptotically AdS massive black holes for  $\kappa < \kappa_{max}$  (red branch) otherwise the geometry displays a naked singularity.

refer to the case without such minimum (blue branch) as type (b1) solution and as type (b2) for the other one (red branch). Recall that for negative mass the relevant sections of the polynomial are the ones running below the  $Y[g] = 0$  axis. The structure of horizons and the type of singularity will be different in both types of branches.

For some region of the space of parameters<sup>16</sup> the extremal minimal mass is not well defined, in the sense that instead of an extremal regular spacetime with a degenerate horizon it has a naked singularity (see for instance figure 9). In that case the temperature also vanishes asymptotically as we decrease the mass. We will not comment on these kind of solutions as they are gravitationally unstable against perturbations [21].

In case we have a well defined extremal negative mass black hole, for (b1) type branches as we increase the mass we always have two (or more) horizons<sup>17</sup>. For type (b2) branches, however, one of the horizons, the inner one, disappears when its radius coincides with the

<sup>16</sup>In particular for that to happen we need  $d = 2K + 1$  and that the branch we are considering does not end at a minimum, i. e. it can only happen for (b1) type solutions in  $d = 2K + 1$ .

<sup>17</sup>One or more for  $\kappa < \kappa_{crit} \equiv -|c_K|$  in the  $d = 2K + 1$  case

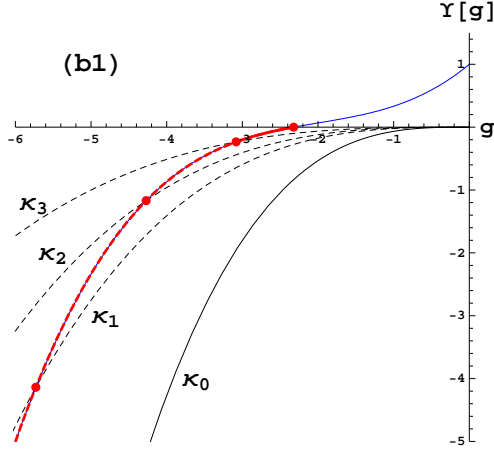


**Figure 9.** EH-branch in cubic Lovelock theory in 7 dimensions for  $\lambda = 0.4$  and  $\mu = 0.2$  (we set  $L = 1$  for simplicity). The dashed curves correspond to  $\kappa (g_+/\sigma)^{\frac{d-1}{2}}$  with hyperbolic topology ( $\sigma = -1$ ) and  $\kappa_0 = -\mu/3 = -2/30$ ,  $\kappa_1 = -0.022$ ,  $\kappa_2 = \lambda = -0.015$ , and  $\kappa_3 = -0.008$ . For masses above  $\kappa_0$  we have just one horizon with no distinction between positive and negative masses. For  $\kappa = \kappa_0$  we have a naked singularity at  $r = 0$  in the same way as for masses below that bound and no extremal state exists.

radius of the singularity, which changes from timelike to spacelike or viceversa. This kind of branch has then a critical value for the mass where the number of horizons changes. This cannot be observed by an outside observer and then both kinds of spacetimes are exactly indistinguishable from this point of view. Figure 10 shows both kinds of solutions in GB gravity,  $\lambda < 0$  and  $\lambda > 0$  for (b1) and (b2) types respectively.

Both classes of branches may in principle have several horizons in the presence of inflection points. The (b1) type branches will always have an even number of horizons except when  $\kappa \geq c_K$  where the smallest horizon disappears. Thus, the singularity at  $r = 0$  is timelike below this critical mass and spacelike above it. The same change of behavior for the singularity appears in the other type of branches with the only difference of the critical mass being set by the minimum,  $\kappa_*$ . In the same way as described for spherical black holes in the EH-branch the couples of horizons appearing or disappearing as function of the mass  $\kappa$  translate into discontinuous changes on the temperature as we vary this parameter. As in the EH-branch, this possibility of having several extremal solutions in one branch amounts to several ground states for different ranges of (negative) black hole masses, with possible transitions among them. At zero temperature, in this case, one does not have a thermal vacuum to compare with contrary to what happens at finite temperature. The negative mass black holes are the preferred phase in that regime.

### 4.3 dS branches

In the same way as the EH-branch these branches can end up at a maximum (b) or extend all the ways to  $r = 0$  (a), red and green branches on figure 11 respectively.

In this last case, the existence of black hole horizons (besides the cosmological one) will again set a series of constraints both on the topologies of the horizon one may consider

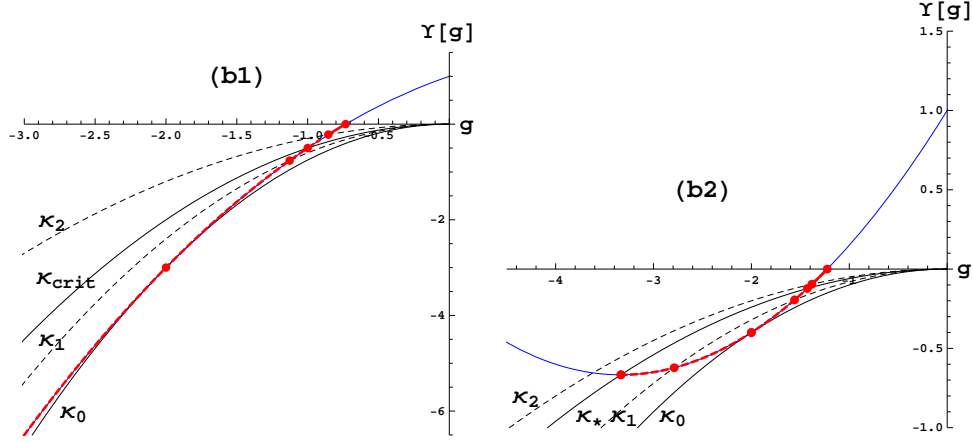


**Figure 10.** EH-branch in GB gravity in 5 dimensions for  $\lambda = -1/2$  and  $\lambda = 0.15$  respectively (we set  $L = 1$  for simplicity). The dashed curves correspond to  $\kappa(g_+/\sigma)^{\frac{d-1}{2}}$  with hyperbolic topology ( $\sigma = -1$ ) and  $\kappa_0 = -0.75$ ,  $\kappa_1 = -0.6$ ,  $\kappa_{\text{crit}} = \lambda = -0.5$ , and  $\kappa_2 = -0.3$  in the first figure and  $\kappa_0 = -0.1$ ,  $\kappa_1 = -0.08$ ,  $\kappa_* = -0.06$  and  $\kappa_2 = -0.05$  in the second. In both cases we have two horizons for  $\kappa_0 < \kappa < \kappa_*$  and one for  $\kappa_* < \kappa$ . For  $\kappa = \kappa_0$  we have a degenerate horizon. In 5 dimensions the singularity becomes naked for  $\kappa \leq \lambda - 1/4$  in both cases. In higher dimensions the behavior is qualitatively the same. For the (b2) type branches the singularity is always located at  $r_* = L\sqrt{-2\lambda}$  while it is at the origin in the (b1) case.

asympt.	$\sigma = -1$	$\sigma = 0$	$\sigma = 1$
dS			

**Table 4.** Taxonomy of the dS branches.

as in the possible values for the mass parameter,  $\kappa$ . For hyperbolic or flat horizons, the metric function  $f$  is always negative and the solution describes a big crunch. For  $\sigma = 1$  the solution may still describe a big crunch if we consider a high enough mass, above the Nariai mass. The difference with respect to Einstein-Hilbert gravity is that in this case one may have several Nariai masses, the big crunch geometry appearing for values of  $\kappa$  above the biggest one. Below that extremal mass at least two horizons exist (an even number for some range of masses), the biggest one corresponding to a cosmological horizon and the following to the black hole horizon. Then we can have two situations. For (b) type branches, at some point the smallest (inner) black hole radius coincides with the radius of the singularity,  $r_- = r_*$  and below that mass the number of horizons changes from even to odd. If close to that critical mass the black hole has just one horizon a naked singularity shows up. The naked singularity always shows up as we decrease the mass of the black

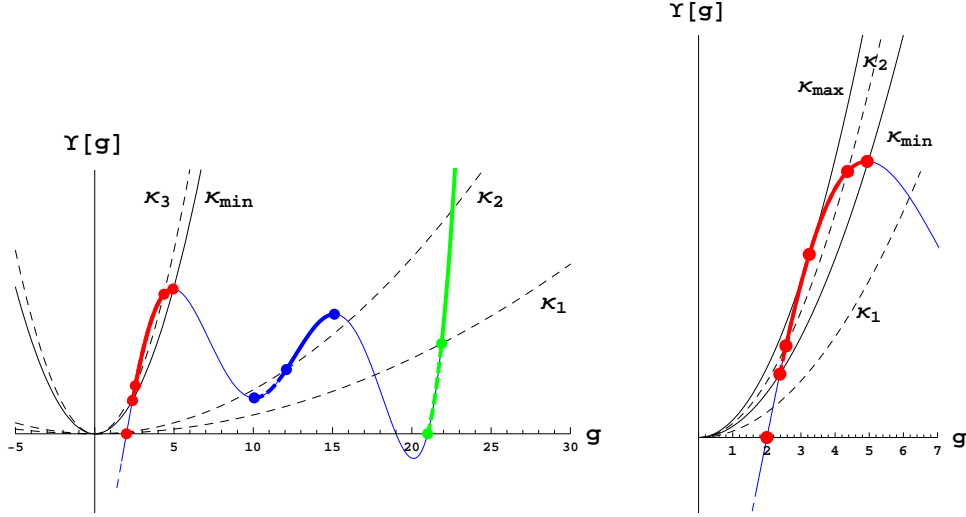


**Figure 11.** Generic features of dS branches are captured in these figures. The different sections of the polynomial qualitatively represent (b) type (in red), excluded (in blue) and (a) type dS branches (in green). There are asymptotically dS massive black holes for  $\kappa_{\min} < \kappa < \kappa_{\max}$  (red branch). The right figure zooms on the (red) dS branch showing that for  $\kappa = \kappa_2 > \kappa_{\min}$  the black hole has outer and inner horizons, while there is a maximum value  $\kappa_{\max}$  at which they coincide, the black hole becoming extremal. For  $\kappa$  not belonging to this range, the red branch displays a naked singularity. Even though the green branch does not seem to have a black hole horizon it always exists for  $d > 2K + 1$  and, in most cases, for some range of masses also in the  $2K + 1$  dimensional case. In some cases for the latter dimensionality just the cosmological horizon exists.

hole. For  $\kappa = c_K$  some other horizons may exist but they will disappear for some lower mass.

For (a) type branches the same happens for  $d = 2K + 1$  just changing the critical mass associated with the maximum by  $\kappa_* \equiv c_K$ . Again, we cannot avoid the nakedness of the singularity as we approach arbitrarily low masses. Therefore the existence of horizons sets for dS branches in these cases two bounds for the mass. Above the upper bound the geometry is a big crunch with a spacelike singularity whereas below the lower bound it has a naked timelike singularity. For  $d > 2K + 1$  (a) solutions the black hole horizon will always exist all the way down to zero mass and just the (upper) Nariai bound for the mass parameter exists.

For  $d = 2K + 1$  another situation that we may encounter is that the singularity is naked for all values of the mass below a certain critical one. The cosmological is the only horizon and it disappears for the critical mass leaving a big crunch geometry behind. No Nariai solution exists in this case. This is the symmetric situation to the non-existence of extremal negative mass black hole discussed earlier for AdS branches.

Again, as for the other cases with spherical topology (and for negative mass AdS solutions), the variation of the number of horizons as a function of  $\kappa$  may translate into discontinuities in the temperature as a function of the mass. This has the same interpretation as in the EH-branch.

## 5 Heat capacity and local thermodynamic stability

The details of the solutions and the behavior of their associated thermodynamic quantities strongly depend on the particular case under consideration. Therefore, a general thermodynamic analysis is highly cumbersome. However, once we have described the qualitative features of the different branches of solutions that we can construct, much and very interesting information can be extracted, most of it arising as universal features of these black hole solutions.

For positive mass black holes, the sign of the heat capacity on a BD stable branch, because of (3.22), depends just on  $\frac{dT}{dr_+}$  which can be written as

$$\frac{dT}{dr_+} = -\frac{g_+}{2\pi} \left[ (d-2) - \frac{d-1}{2} \frac{\Upsilon[g_+]}{g_+ \Upsilon'[g_+]} \left( 1 + 2g_+ \frac{\Upsilon''[g_+]}{\Upsilon'[g_+]} \right) \right], \quad (5.1)$$

where the second term (in brackets) seems to be related to the shear potential felt by perturbations in the shear channel [21].

We did not manage to check the classical stability in full generality, but in the regimes of *high* and *low* masses.<sup>18</sup> We will just consider horizonful solutions as they are the only ones with associated thermodynamic variables. Then, we will have hyperbolic AdS branches; hyperbolic, flat and spherical EH-branches and spherical dS branches, classified in different subclasses (see table 1).

The simpler case to analyze is that of toroidal or planar black holes, that imply that we must consider just the EH-branch. The thermodynamic variables, in that case, do not receive any correction from the higher curvature terms in the action and the expression reduces to the usual formula of Einstein-Hilbert gravity,

$$\frac{dT}{dr_+} = \frac{d-1}{4\pi L^2}, \quad (5.2)$$

This expression is positive. Therefore, the black hole is locally thermodynamically stable for all values of the mass (equivalently, of  $r_+$ ).

For the EH-branch, the only one admitting all three topologies, the situation is exactly the same for  $\sigma = \pm 1$  in the large mass limit. In these cases, the value of  $g$  at the horizon  $g_+ = \sigma/r_+^2$ , asymptotically approaches zero from both sides, and again the formulas reproduce the planar case. Einstein-Hilbert gravity captures the universal thermodynamic description of Lovelock black holes with large enough mass<sup>19</sup>. EH-branch's black holes in this regime are then always stable.<sup>20</sup> It is worth recalling here that for sufficiently large mass just the EH-branch defines a horizonful black hole, the other branches describing geometries with naked singularities or big crunch spacetimes.

<sup>18</sup>There is another source of instability due to perturbations of the black hole solutions. Earlier relevant work on this issue includes [60–66].

<sup>19</sup>It does not capture other features in this regime, for instance related to the stability and causality preserving properties of the solutions [12, 13, 67].

<sup>20</sup>This is also the case for a special class of (maximally degenerated) Lovelock theories whose analysis is actually not considered in the present article. Those theories admit a single (EH-)branch of black holes [68]. The results there also coincide with the generic analysis for spherical black holes presented here.

As we decrease the mass, particular features of the different topologies pop up and we need to consider them separately. For  $\sigma = -1$ , the small mass limit corresponds to a smooth deformation of the vacuum, also in what concerns the black hole horizon. In that regime the second term inside the brackets of (5.1) is negligible,  $\Upsilon[g_+] \approx \Upsilon[\Lambda] = 0$ , and the expression approaches

$$\frac{dT}{dr_+} \approx \frac{d-2}{2\pi} (-g_+). \quad (5.3)$$

Therefore, as  $g_+ < 0$  in this case, the low mass black holes are also stable. Even if both extrema of the spectrum for hyperbolic black holes in the EH-branch are stable, one may encounter unstable intermediate phases. This is not the case in GB gravity<sup>21</sup> (see figure 12), where we find that hyperbolic black holes are always locally thermodynamically stable, even if we consider negative masses above the extremal one (depicted in red in the figure). Indeed, the extremal state can be as well shown to be always stable from this point of view.

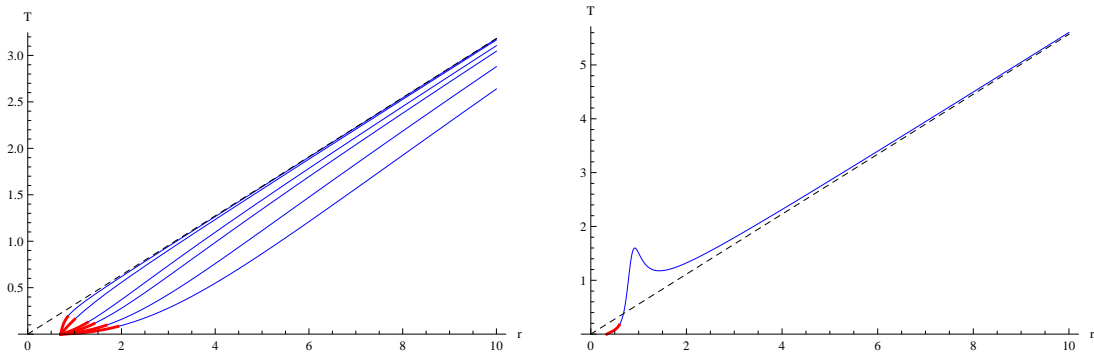


**Figure 12.** Temperature versus horizon radius (equivalently versus black hole mass,  $\kappa$ ) for hyperbolic black holes. The first figure corresponds to GB gravity in  $d = 5$  for  $\lambda = -10, -5, -2, -1, 0, 0.2$  (from bottom to top). The behavior is qualitatively the same in higher dimensions. Such black holes are stable for all values of the mass (even negative, in red). The black dashed line corresponds to the planar case to which all curves asymptote. The second figure corresponds to an example of intermediate unstable phase in cubic Lovelock theory in  $d = 8$  with  $\lambda = 0.65$  and  $\mu = 0.5$ . In all cases we set  $L = 1$  for simplicity.

It has zero temperature and all black holes with higher masses have positive temperature, thus the heat capacity has to be positive close enough to this point.

In some cases, for  $d = 2K + 1$ , this extremal negative mass black hole does not exist. In that situation we may consider, in principle, infinitesimally small black holes,  $r_+ \rightarrow 0$ , with temperatures approaching zero asymptotically. The zero size black hole again fixes a bound in the mass, and black holes close to that bound are stable in the same way as the ones close to the extremal black hole. The problem is that such minimal mass state is singular in this case.

This discussion also applies, on general grounds, to AdS branches with hyperbolic horizons. The only difference is that it exists in general a maximal mass for which the

<sup>21</sup>Contrary to what is stated in [46]; the negative specific heat found there corresponds to inner horizons and, thus, does not indicate any instability of the system.

temperature diverges. Thus, close enough to that point the heat capacity has necessarily to be positive and the black hole thermodynamically stable. This can be seen directly from (5.1), as long as the heat capacity close to the maximum approaches the positive value

$$\frac{dT}{dr_+} \approx \frac{d-1}{2\pi} g_+ \frac{\Upsilon[g_+] \Upsilon''[g_+]}{\Upsilon'[g_+]^2}, \quad (5.4)$$

diverging as well when we reach the critical mass.  $\Upsilon[g_+]$  and  $\Upsilon'[g_+]$  are positive due to positivity of the mass and the avoidance of BD instabilities. The second derivative  $\Upsilon''[g_+]$  is negative as we are close to a maximum and also  $g_+$  is negative as we are in an AdS branch with  $\sigma = -1$ . The plot of temperature versus horizon radius will be in general qualitatively similar to that corresponding to the EH-branch, with the difference that the temperature diverges at some finite value of  $r_+$ .

For spherical black holes the discussion is a bit more complicated and we have to distinguish different cases. For the EH-branch we distinguish two different subclasses, types (a) and (b) depending, respectively, on whether the branch continues until infinity or it ends up at a maximum. In the first case we can define a small black hole limit for that branch,  $r_+ \rightarrow 0$ , and this may correspond respectively to finite or zero mass for  $d = 2K + 1$  and  $d > 2K + 1$ . In that regime, in the latter case,

$$\frac{dT}{dr_+} \approx -\frac{d-2K-1}{4\pi K} g_+ < 0, \quad (5.5)$$

thus the black hole is thermodynamically unstable in exactly the same way as in the usual Einstein-Hilbert gravity. The situation changes for  $d = 2K + 1$ , where the temperature vanishes asymptotically. Therefore, small black holes are stable in odd dimension for the highest order Lovelock gravity,<sup>22</sup> whereas they are unstable in all other cases. For (b) type branches something similar happens as we approach the minimal mass set by the maximum. At this critical mass the temperature again diverges, but in this case as we lower the mass. The heat capacity is negative, as we can also infer from (5.4), taking into account that  $g_+$  has a positive value in the case under consideration. Black holes close enough to this minimal mass one are then unstable. This kind of behavior can be seen for instance in GB gravity (see figure 13).

There is one further possibility that has not been included in the discussion of the previous paragraph. It is the case in which the form of the polynomial is such that it allows for more than one black hole horizon. Then, either for (b) type as well as (a) type solutions (in  $d = 2K + 1$  dimensions), we may still have horizons covering the singularity for some range of masses below the one set by the maximum. As we lower the mass further we then encounter at least one extremal black hole. This black hole will be stable in the same way that it is the extremal hyperbolic black hole of negative mass. One such case is shown in figure 14, that corresponds to the cubic polynomial plotted in figure 2. In general, we may also have unstable regions in between the two stable ones. This situation does not decisively depend on the dimension and, for instance, the same behavior is observed in eight dimensions. This case has features of the previously discussed spherical black holes but

---

<sup>22</sup>In particular we need  $c_K > 0$  for type (a) EH or dS branches to exist.

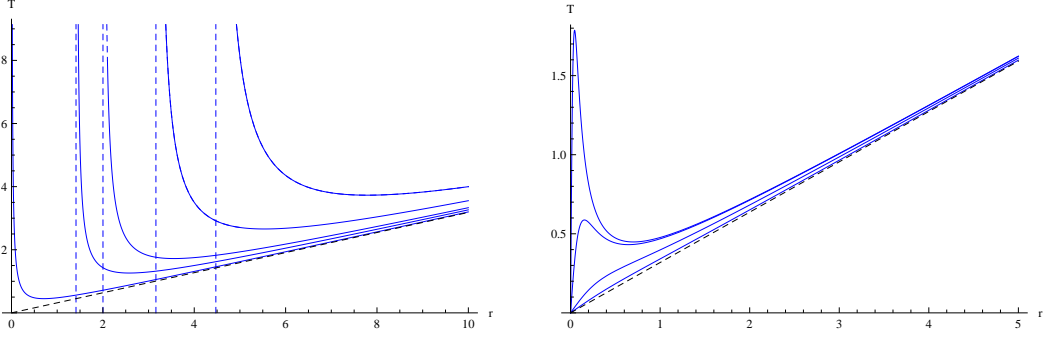


**Figure 13.** Temperature versus horizon radius (equivalently versus black hole mass,  $\kappa$ ) for spherical black holes in  $d = 5$  GB gravity. The first figure corresponds to negative values of the GB coupling,  $\lambda = -10, -5, -2, -1, 0$  (from top to bottom), whereas the second considers positive values,  $\lambda = 0.001, 0.01, 0.1, 0.2$  (from top to bottom). We set  $L = 1$  for simplicity. The dashed blue lines indicate the value of the mass for which the temperature diverges and which is set by the maximum. We observe the appearance of a new stable phase for small positive values for  $\lambda$  and even the disappearance of the unstable region for high enough  $\lambda$ . This stable region of small black holes disappears in higher dimensions, the qualitative behavior being similar to the  $\lambda = 0$  case for all positive values of  $\lambda$ .

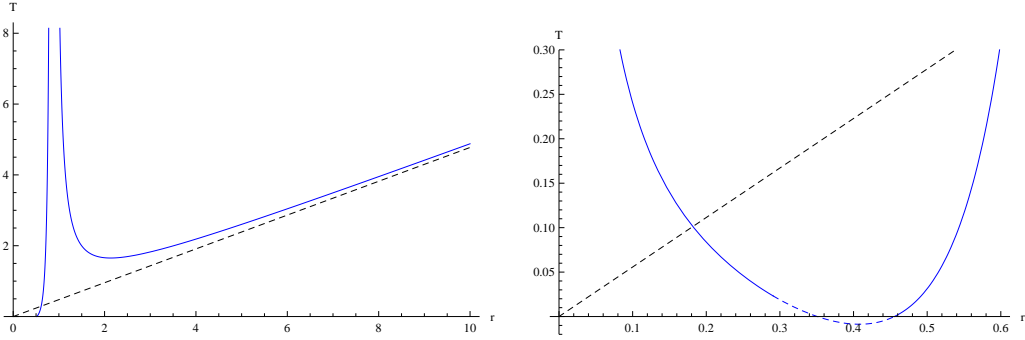


**Figure 14.** Temperature versus horizon radius (equivalently versus black hole mass,  $\kappa$ ) for spherical black holes in  $d = 7$  (figure on the left) cubic Lovelock gravity with values for the couplings  $\lambda = -0.746$ ,  $\mu = 0.56$  and  $L = 1$ . Remark that the black hole reaches zero temperature with finite (positive) mass. For  $d = 8$  (on the right) the shape of the curve is qualitatively the same except in the low radius region where a new branch of black holes with diverging temperature appears. We just show a zoom of the left bottom corner. We can also verify the existence of the temperature (and radius) jump commented in the main text. The dashed line correspond to inner horizons, one of them becoming outer for masses below the extremal one.

its behavior is similar to the (negative mass) hyperbolic black holes close to the extremal state.

A very similar discussion applies to the low mass regime of the other possible spherical solutions, the ones corresponding to dS branches. The high mass regime is however very different in this case. These black holes may increase their mass until they reach a maximal (so-called *Nariai*) mass, which is set by the shape of the polynomial. This is an extremal state and, as we reach it from lower mass configurations, the system is thermodynamically

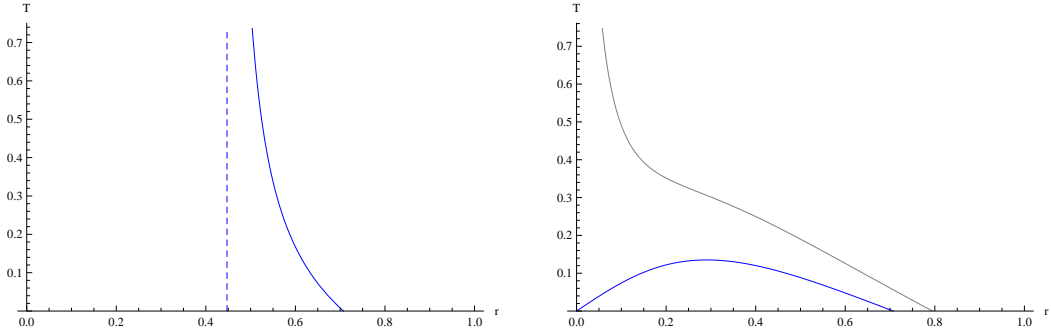


**Figure 15.** Temperature versus horizon radius (equivalently versus black hole mass,  $\kappa$ ) for spherical black holes in  $d = 5$  GB gravity with positive cosmological constant,  $L^2 = -1$  (in blue). The first figure,  $\lambda = -0.1$ , corresponds to a type (b) dS branch. We can identify the zero temperature state in the high mass regime with the Nariai solution whereas the temperature diverges as we approach the maximum in the opposite regime. The dashed blue lines indicate the value of the mass for which the temperature diverges and which is set by the maximum. For positive values of the coupling,  $\lambda = 0.1$  in the second figure, what corresponds to a type (a) dS branch one may identify again the extremal state at the maximal mass with the Nariai solution but in this case the temperature also goes to zero in the opposite regime, as the radius of the black hole decreases. Remark that the zero radius black hole has finite mass in this case. For higher dimensions the new stable region of small black holes disappears (the gray line corresponds to  $d = 6$ ) and this spherical black holes are also everywhere unstable as their type (b) counterparts, the only difference being that the temperature diverges in the zero mass limit in this case.

unstable close to it. Then, the low mass regime is the same as for the spherical EH-branch, whereas the high mass regime is unstable and leads to an extremal black hole with zero temperature. We may construct dS branches of types (a) and (b) using GB gravity with positive cosmological constant (we just set  $c_0 = -L^2$ ). In this case, the (b) type branch (figure 15, left) is unstable for all allowed values of the mass whereas, since we are considering  $d = 5$  (which is  $d = 2K + 1$  in this case), while a stable region of small black holes appears for (a) type branches (figure 15, right). This stable region disappears in higher dimensions. In general, spherical dS branches may have some stable intermediate region, but they are unstable (or even inexistent) for high enough temperature.

Let us summarize the main results of this section before pursuing the analysis. For hyperbolic topologies, either for EH or AdS branches, the black hole has always two stable regions, at low and high temperatures. For intermediate temperatures, these solutions may have more than one possible mass (or radius), some of them (or even all of them, depending on the temperature) unstable. The only difference of AdS branches with respect to the EH case is that the high temperature regime has a maximal finite mass in the former.

The spherical solutions exhibit quite different features depending on the kind of branch we consider. From the thermodynamical point of view, we may distinguish those cases where there is a minimal temperature for the black holes to exist from those where this is not the case. In the first case, we do not reach any extremal black hole either in the low or high mass regimes. This correspond to the generic situation in EH-branches. In that case, for temperatures below the above referred minimal one, just the thermal vacuum may exist

whereas, for high enough temperatures, the black hole may exist with two very different masses, one very low (which is unstable) and one very high (stable). For intermediate temperatures close to the minimal value, we may in principle encounter several stable and unstable black holes.

The other type of spherical black holes concern all dS branches and the EH one when it reaches an extremal state at low masses. For these branches, black hole solutions exist for the whole range of temperatures, except in the case where a dS branch reaches an extremal state at low as well as at high masses. For the EH-branch, in this situation, we have two stable phases again, as in the hyperbolic case, one in the low and one in the high temperature regimes. At intermediate temperatures the black hole may have several possible masses, some of them unstable. Spherical black holes have a far richer spectrum of thermodynamic behavior than any other that will be explored elsewhere [21].

The planar case is the most simple one and just captures the high temperature regime of the EH-branch.

## 6 Hawking-Page-like phase transitions

The existence of unstable phases, as well as the existence of several possible black hole solutions for the same temperature, suggest the occurrence of Hawking-Page-like phase transitions, as already observed in the case of Gauss-Bonnet gravity [37, 41]. These phase transitions should be particularly relevant when studying the physics of the dual CFT plasma. In order to analyze this we need to discuss the global stability of the solutions. Any system in thermal equilibrium with an infinite heat reservoir (and thus at constant temperature) will be described by the canonical ensemble, whose relevant thermodynamic potential is the Helmholtz free energy,  $F$ . The preferred, and so globally stable, solution is the one that minimizes  $F$ . For instance, the free energy of the black hole solution calculated in (3.26), is the free energy with respect to the vacuum solution, except for the hyperbolic case where the finite ground state free energy must be subtracted. Therefore, the sign of the free energy determines which solution is globally preferred at any given temperature, the appropriate black hole (if several are possible) or a thermal bath in vacuum.

The general analysis is, again, hard and not very enlightening. We will just concentrate in showing general features of these black hole solutions without entering on the details of the different cases. We will consider the same regimes analyzed for the local stability as there we can easily find the expression for the free energy. In the planar case the analysis is very simple since the free energy reads:

$$F = -\frac{V_{d-2}}{16\pi G} \frac{r_+^{d-1}}{L^2} . \quad (6.1)$$

The black hole is then always the preferred solution, as indicated by the negative sign of the free energy, and no phase transitions occur. This will be the situation in the large mass limit of the other topologies in the EH-branch. As for large enough  $r_+$  the free energy may be as large as one wants, ambiguities on the reference background do not matter in this limit.

## 6.1 Spherical black holes

For spherical black holes, since we have many different possible situations, we will restrict our discussion to the two most generic ones. For EH we will consider separately the case of having a stable low temperature phase (as in  $d = 5$  GB gravity with positive  $\lambda$ ), and the case where a minimal temperature is needed for black hole solutions to exist. The second case is the analog of the usual situation in the Einstein-Hilbert gravity. At low temperatures just the thermal vacuum can be considered as the globally stable solution whereas for higher temperatures two or more black hole solutions are also possible. For high enough temperature just two of them remain. The small one has always positive free energy. For an (a) type branch,

$$F = \frac{(d-2)V_{d-2} r_+^{d-2K-1}}{16\pi G} \frac{1}{d-2K}, \quad (6.2)$$

whereas for the (b) type case the temperature diverges as we approach the maximum  $g_+ \rightarrow g_*$ , and the free energy is approximated by  $F \approx -TS$ . Then, for positive entropy, the small black hole solution has negative free energy and it is stable against the vacuum. However, it is not the minimum of the free energy since the big black hole has always a lower one. This is quite easy to see by realizing that the small black hole entropy goes to a constant as we approach the maximum whereas the entropy grows indefinitely for big black holes, as they approach the planar limit. Thus, the small black holes are not just locally but also globally unstable.

The big black holes however, approach the planar limit and then have in general negative free energy. We have then a Hawking-Page-like phase transition, from the thermal vacuum at low temperatures to big black holes at high temperatures. The difference with respect to the Einstein-Hilbert case is that at intermediate temperatures we may have several black holes, some with positive and other with negative free energy. Recall that the free energy may have up to  $2K - 1$  zeros, that is, it can change sign  $2K - 1$  times. It is important that it is an odd number of times as it has different sign for small and big black holes. For ranges of temperature where several black holes have negative free energy also transitions among them may happen, the globally preferred solution being, as always, the one with the lowest free energy. This would be an example of a new kind of phase transition, different from the Hawking-Page one, where one of the phases is always the thermal vacuum. Further research on this possibility is currently under scrutiny [21].

If the EH-branch has stable low temperature black holes, *i.e.*, for type (a) in  $d = 2K + 1$ , these solutions are again globally unstable as indicated by their positive free energy that asymptotes a constant when  $r_+ \rightarrow 0$ ,

$$F = \frac{(d-2)V_{d-2}}{16\pi G}. \quad (6.3)$$

This is very similar to the earlier formula (6.2), though in this particular case. The same happens for the possible extremal black holes that one may encounter as well for (a) as for (b) type EH-branches. In the limit of low temperatures the free energy coincides with the mass and, as such states have positive mass, they are globally unstable. The globally

preferred phase is the thermal vacuum which is the minimal mass solution. Then, again one has the same kind of transition as described in the previous paragraph.

In the global analysis one should in principle consider these extremal solutions for all temperatures [69],<sup>23</sup> as long as they can be identified with an arbitrary period in imaginary time avoiding any singularity. In the large temperature limit, as we said before, the free energy approaches  $F \approx -TS$  and so the globally stable solution is the one with the biggest entropy. For a given branch, the entropy increases with the radius and the biggest radius black hole will be the preferred phase. Then, these extremal solutions do not change the conclusions of the analysis even though they may play a role at intermediate temperatures.

Another situation we did not comment at length is the possibility of having negative entropy at the maximum. This happens already in the simplest possible case. In GB gravity, for negative  $\lambda$ , we have a maximum in the EH-branch situated at  $g_\star = -1/2\lambda$ . At that point the entropy is

$$S_\star = \frac{A}{4G_N} \left( 1 + 2\lambda \frac{d-2}{d-4} g_\star \right) = -\frac{A}{2(d-4)G_N} < 0. \quad (6.4)$$

As pathological as it may seem, the consequence of this from the global stability point of view is clear. The solution is unstable for spherical black holes with masses close to the critical one (given implicitly by  $g_+ = g_\star$ ), as all contributions for the free energy are positive. The same happens for zero entropy where the free energy is just the mass. Again, the globally preferred solution is the big black hole one as before and the discussion goes through.

For dS branches the situation at low mass is exactly the same, with globally unstable low or high temperature black holes. In this case when the free energy of these black holes is negative close to a maximum, we still have a solution to which compare. The biggest black hole in this case is a Nariai solution that, being extremal, we may associate to any given temperature [69]. Again as the entropy always grows with the radius, the Nariai solution has lower free energy and thus it is globally preferred at high temperature, even though it is locally unstable. This is a pathological behavior that is presumably telling us that there is another solution that escapes from our analysis (for instance, a less symmetric black hole). In the case where the analyzed branch displays several possible Nariai solutions, the globally preferred one is the most massive, as it has the biggest radius. At temperatures close to zero the free energy however approaches the value of the mass and then the globally stable phase is always thermal vacuum as long as any other possible solution has positive mass and free energy. We have a seemingly different kind of Hawking-Page phase transition where the high temperature phase corresponds to a Nariai solution.<sup>24</sup>

---

<sup>23</sup>This has been disputed by some authors (see [58] for instance) in reason of the semiclassical instability of these solutions.

<sup>24</sup>In case the Nariai solution is just valid for thermal equilibrium at zero temperature, we face two possibilities. For (a) type branches the preferred phase in the high temperature limit would be just the thermal vacuum and no Hawking-Page-like phase transition seems to occur. For (b) type branches with positive entropy the globally stable solution would be the near-critical black hole approaching the maximum of the polynomial.

As discussed in the previous section for the EH-branch, one may encounter negative values of the entropy at the maximum<sup>25</sup>. This does not change the conclusion concerning the instability of the small black holes as it makes them unstable even compared to the vacuum. However, the entropy may, in some cases be also negative for the Nariai solution (for the biggest one) and in this case this solution is globally unstable the thermal vacuum being the preferred phase. The same applies if the Nariai solution has zero entropy. We do not seem to have a phase transition in this case, but if the Nariai solution which is the biggest black hole has negative entropy, every solution in that branch has negative entropy as well. This situation is obviously pathological and should be discarded. The thermal vacuum is the preferred phase for all temperatures in that case. This happens in the GB theory with negative coupling and positive cosmological constant.

## 6.2 Hyperbolic black holes

The case of hyperbolic black holes is more speculative and it actually shows some pathological features and interpretation problems as we shall comment. For these solutions one may compute the free energy at the high and low temperature regimes as in previous cases. As the maximally symmetric space has temperature in this case it is not clear how to use it as a ground state. Instead we will consider the extremal negative mass black hole that can be identified with any given temperature.<sup>26</sup>

For the EH-branch in the high temperature regime we just have one possible black hole solution. It has negative free energy as it approaches the planar limit and so it is globally preferred to any reference state. The same happens for the AdS branches, that end up at a maximum of the polynomial. As we approach the critical mass for which the singularity becomes naked,  $g_+ \rightarrow g_*$ , the free energy approaches  $F \approx -TS$  that is arbitrarily negative for positive entropy. For negative entropy at the maximum, which corresponds to the biggest possible black hole in the AdS branch, every black hole has negative entropy and this situation must be excluded as pathological. In this case even the would be negative mass ground state has negative entropy. The meaning of this if any is unclear.

At high temperatures the black hole is then the preferred phase independently of the ground state we consider, as long as the free energy can take arbitrarily large negative values. For lower temperatures we have to consider black holes close to the extremal one (or ones)<sup>27</sup>. In the zero temperature limit just these extremal states matter and their free energy is given just by the mass. Then, the globally preferred phase in that limit is the lowest mass state. For slightly higher temperatures one expects that the globally preferred

---

<sup>25</sup>If the entropy is positive at the maximum, minimal radius of the EH or dS spherical branch, it is positive for the whole branch as it is a growing function of the horizon radius. For (a) type branches, the entropy is always positive as it is zero in the zero radius limit.

<sup>26</sup>If we consider this is not possible the analysis is trivial with just (one or more) black hole solutions no matter the value of the temperature. No Hawking-Page-like phase transitions occur in this case, just the possibility of transitions among black holes of different masses.

<sup>27</sup>In the cases where such a state does not exist we have to consider the limit in which the horizon and the singularity merge that also has vanishing temperature limit. For the discussion remark that this singular solution has vanishing entropy and thus its free energy does not change as we increase its temperature, it is just the mass.

solution is still described by the same minimal mass extremal state (identified with finite temperature) or the corresponding black hole solution that is just a smooth deformation of it. It is however hard to elucidate in general which of both solutions has the lowest free energy, and then the existence or not of Hawking-Page-like phase transitions. One may also expect transitions between ground states (and the corresponding low temperature black holes) as we increase the temperature. As not all these extremal states have the same entropy, the free energy of these solutions changes with temperature and the relative stability of them will in general change as well. This does not however correspond to a Hawking-Page-like phase transition as as such we just consider a transition between state with and without black hole, what in the framework of AdS/CFT is interpreted as a confinement-deconfinement phase transition. The interpretation of this new kind of phase transitions is unclear in that context.

To sum up, we always have Hawking-Page-like phase transitions for spherical black holes in the EH and dS branches. In the latter case the transition may be avoided if the entropy of the black hole solutions is negative or the Nariai solution is just considered for vanishing temperature in which case we have just the thermal vacuum. In the planar case we have the opposite situation where the black hole is always the globally preferred case. Finally, for hyperbolic black holes the high temperature preferred phase is always the black hole as in the planar limit but the opposite regime is unclear. We cannot elucidate in general whether the lowest free energy corresponds to the extremal state at finite temperature or to the corresponding black hole solution, as one is just a smooth deformation of the other. In addition to this, in the cases with several extremal negative states phase transitions among them are in principle possible.

## 7 Discussion

In this paper we presented a novel approach to deal with the full classification and description of black hole solutions with constant curvature horizons in Lovelock gravity. Our proposal allows to treat the generic case where the whole set of Lovelock coupling constants is arbitrary, contrary to most studies existing in the literature where the analysis is restricted to particular cases. Most of these cases, moreover, correspond to degenerate vacua of Lovelock gravity, while our approach is valid in general and is most useful in the non-degenerate case.

We discussed the main features of all possible configurations. In particular, we have established a recipe to scrutinize the number of horizons and their evolution with the mass, something that we expect to be useful to visualize and gain intuition in physical processes involving black holes in such theories: evaporation, mass accretion and appearance of naked singularities [21].

We presented some general features of Lovelock black holes' thermodynamics, analyzed their local and global stabilities and the possible existence of phase transitions. Even if these solutions show some seemingly pathological features, such as negative values for the entropy, these are avoided if we restrict ourselves to the globally preferred phase. Just for

the hyperbolic black holes, in some regions of the parameter space, also the reference or ground state has negative entropy. The meaning of this is unclear.

Global stability always selects, in the high temperature regime, the biggest black hole solution, as it is the one with biggest entropy (and the less likely to be negative). If we apply the same criterium to all possible solutions, regardless of the branch to which they belong, the selected solution is always the one approaching the planar limit, since it is the only one that has arbitrarily big entropy. The comparison of solutions belonging to different branches is not really allowed as they have different asymptotics. The usual euclidean prescription says that we must compare all solutions *with the same boundary conditions* what certainly includes the asymptotics. However the existence of spherical shock wave solutions [70] separating regions corresponding to different vacua suggest the possible existence of mixed solutions and transitions between branches. In that context, the high temperature phase would always correspond to the universal planar limit. From a holographic point of view, this is consistent with the intuitive idea that effects due to the curvature of spacetime, being overcome by finite temperature effects, are negligible for field theory calculations. This is a new way of addressing the multivaluedness problem of Lovelock theories.

The usual Einstein-Hilbert gravity admit in principle topological solutions displaying naked singularities. These may arise as a result of a bad choice of topology or as associated to negative mass, below the extremal one for hyperbolic horizons. The latter are just a special case of *trans-extremal* solutions, where the values of the parameters are chosen in such a way that, an otherwise well defined black hole solution with positive temperature, is beyond the extremal state. Example of this is just the Reissner-Nordstrom black hole or the negative mass hyperbolic black holes. In principle, all these situations are ruled out by the cosmic censorship conjecture that states that naked singularities do not form in the evolution of generic initial conditions. For instance, the evaporation process for black holes with several horizons should stop at the extremal state as it has zero temperature and this avoids the formation of trans-extremal solutions in that case.

The situation in generic Lovelock theories of gravity is rather different. For this wide family of gravity theories, as we have seen analyzing the case of static uncharged black holes, there are several situations that suggest a possible violation of the cosmic censorship conjecture. In addition to the cases pointed out in the previous paragraph, new kinds of naked singularities appear, some of them seem naively to be formed in the evolution of these black holes. This can happen both for the otherwise seemingly well-behaved Einstein-Hilbert branch and it certainly happens generically on the extra 'higher order' branches.

Many of these naked singularities arise because the branch of interest ends up at a maximum or a positive (for positive mass) minimum of the Lovelock polynomial. The existence of a minimum cutting off the branch as we go to large values of the radial coordinate corresponds to a complex cosmological constant associated with this particular branch. The maxima, in turn, appear in a variety of cases. They set a maximal mass on AdS branches with hyperbolic topology (there is no way to avoid the naked singularity for the other topologies). Also, they set a minimal mass in some EH or dS branches with spherical topologies. Large mass or other topologies do not lead to naked singularities but

to big crunch geometries.

The other possibility for naked singularities to appear is just the spherical case in the maximal  $d = 2K + 1$  Lovelock theory, for the Einstein-Hilbert or any of the asymptotically dS branches when they extend all the way to  $r = 0$  without encountering any singularity (maxima or minima). In those cases we find a naked singularity for masses below a critical value,  $\kappa_{\text{crit}}$ . Any other possible naked singularity may be considered in the same class as the ones appearing in Einstein-Hilbert gravity.

As we think of the evolution of the black holes studied in the present paper, we realize that naked singularities seem to easily form, at least naively. Consider for instance the evaporation of spherical black holes. For (b) type EH or dS branches these black holes always reach a critical mass where the horizon coincides with the singularity. At that point the temperature diverges but a finite mass naked singularity remains. The naked singularity inevitably form. We emphasized the word naively before as in the present analysis we just considered the thermodynamic stability of the solutions. These solutions are locally and globally unstable, however they are still valid solutions that may form under evolution of generic spherically symmetric initial conditions. A more general analysis is needed to elucidate whether naked singularities may form or not in these theories [21].

We have fixed, throughout this paper, the values of the cosmological constant and the Newton constant appearing in the lagrangian to their customary values in AdS Lovelock gravities. It is worthwhile mentioning that a straightforward generalization of this work amounts to studying the case of dS Lovelock theories (note that there are AdS vacua also in this case), as well as theories where the Newton constant has negative sign. On the one hand, we shall mention that this sign flip was already considered in the context of three dimensional topologically massive gravity, where it was found that a negative Newton constant is useful to render otherwise negative energy modes harmless for the stability about flat space [71]. Furthermore, in higher dimensions, even though  $G_N < 0$ , the generic structure of branches discussed in this paper will remain, and there will always be solutions corresponding to well-defined gravities with positive cosmological constant.

In the last few months there were some papers constructing gravitational theories that share some compelling properties with Lovelock lagrangians [72, 73]. In particular, these are lower dimensional theories displaying black hole solutions whose profile precisely correspond to Lovelock black holes [74]. Some of the results of this paper are of direct application to those cases as well. This is particularly interesting due to the fact that quasi-topological gravities are higher curvature theories in dimensions lower than their corresponding Lovelock cousins, thus the results are of interest in more ‘physical’ setups of AdS/CFT [75].

Lovelock theories have the remarkable feature that lots of physically relevant information is encoded in the characteristic polynomial  $\Upsilon[g]$ . Boulware-Deser-like instabilities, for instance, can be simply written as  $\Upsilon'[\Lambda] < 0$ , which has a beautiful CFT counterpart telling that the central charge,  $C_T$ , has to be positive to avoid this instability. Now,  $\Upsilon'[\Lambda]$  can be thought of as the asymptotic value of the quantity  $\Upsilon'[g]$  that is meaningful in the interior of the geometry, and has to be positive all along the corresponding branch. Naked singularities taking place at extremal points of the polynomial are suggestive of the fact

that  $\Upsilon'[g]$  should be a meaningful entry of the holographic dictionary (see [18] for related ideas) that does not exist in the case of Einstein-Hilbert gravity.

We hope to report on some of these interesting open problems elsewhere.

## Acknowledgements

We would like to thank Andrés Gomberoff, Hideki Maeda, Julio Oliva, Miguel Paulos, Ricardo Troncoso and Jorge Zanelli for their interesting comments. XOC wishes to thank the Perimeter Institute for its kind hospitality where part of this research was performed. XOC is supported by a spanish FPU fellowship. He is thankful to the Front of Galician-speaking Scientists for encouragement. This work is supported in part by MICINN and FEDER (grant FPA2008-01838), by Xunta de Galicia (Consellería de Educación and grant PGIDIT10PXIB206075PR), and by the Spanish Consolider-Ingenio 2010 Programme CPAN (CSD2007-00042). The Centro de Estudios Científicos (CECS) is funded by the Chilean Government through the Millennium Science Initiative and the Centers of Excellence Base Financing Program of Conicyt, and by the Conicyt grant Southern Theoretical Physics Laboratory ACT-91. CECS is also supported by a group of private companies which at present includes Antofagasta Minerals, Arauco, Empresas CMPC, Indura, Naviera Ultragas and Telefónica del Sur.

## References

- [1] D. Lovelock, *The Einstein tensor and its generalizations*, *J. Math. Phys.* **12** (1971) 498–501.
- [2] B. Zwiebach, *Curvature Squared Terms and String Theories*, *Phys. Lett.* **B156** (1985) 315.
- [3] J. M. Maldacena, *The large  $N$  limit of superconformal field theories and supergravity*, *Adv. Theor. Math. Phys.* **2** (1998) 231–252, [[hep-th/9711200](#)].
- [4] I. R. Klebanov and E. Witten, *Superconformal field theory on threebranes at a Calabi-Yau singularity*, *Nucl. Phys.* **B536** (1998) 199–218, [[hep-th/9807080](#)].
- [5] A. M. Polyakov, *The wall of the cave*, *Int. J. Mod. Phys.* **A14** (1999) 645–658, [[hep-th/9809057](#)].
- [6] A. Strominger, *Black hole entropy from near horizon microstates*, *JHEP* **9802** (1998) 009, [[hep-th/9712251](#)].
- [7] J. D. Brown and M. Henneaux, *Central charges in the canonical realization of asymptotic symmetries: an example from three-dimensional gravity*, *Commun. Math. Phys.* **104** (1986) 207–226.
- [8] E. Witten, *Conformal Field Theory In Four And Six Dimensions*, [arXiv:0712.0157](#).
- [9] J. de Boer, M. Kulaxizi, and A. Parnachev, *AdS<sub>7</sub>/CFT<sub>6</sub>, Gauss-Bonnet Gravity, and Viscosity Bound*, *JHEP* **03** (2010) 087, [[arXiv:0910.5347](#)].
- [10] X. O. Camanho and J. D. Edelstein, *Causality constraints in AdS/CFT from conformal collider physics and Gauss-Bonnet gravity*, *JHEP* **04** (2010) 007, [[arXiv:0911.3160](#)].
- [11] A. Buchel, J. Escobedo, R. C. Myers, M. F. Paulos, A. Sinha, and M. Smolkin, *Holographic GB gravity in arbitrary dimensions*, *JHEP* **03** (2010) 111, [[arXiv:0911.4257](#)].

- [12] X. O. Camanho and J. D. Edelstein, *Causality in AdS/CFT and Lovelock theory*, *JHEP* **06** (2010) 099, [[arXiv:0912.1944](#)].
- [13] J. de Boer, M. Kulaxizi, and A. Parnachev, *Holographic Lovelock gravities and black holes*, *JHEP* **06** (2010) 008, [[arXiv:0912.1877](#)].
- [14] D. M. Hofman and J. Maldacena, *Conformal collider physics: Energy and charge correlations*, *JHEP* **05** (2008) 012, [[arXiv:0803.1467](#)].
- [15] A. Buchel and R. C. Myers, *Causality of Holographic Hydrodynamics*, [arXiv:0906.2922](#).
- [16] D. M. Hofman, *Higher Derivative Gravity, Causality and Positivity of Energy in a UV complete QFT*, *Nucl. Phys.* **B823** (2009) 174–194, [[arXiv:0907.1625](#)].
- [17] M. Brigante, H. Liu, R. C. Myers, S. Shenker, and S. Yaida, *Viscosity Bound Violation in Higher Derivative Gravity*, *Phys. Rev.* **D77** (2008) 126006, [[arXiv:0712.0805](#)].
- [18] M. F. Paulos, *Holographic phase space: c-functions and black holes as renormalization group flows*, [arXiv:1101.5993](#).
- [19] H. Maeda, S. Willison, and S. Ray, “Lovelock black holes with maximally symmetric horizons,” to appear.
- [20] B. Zumino, *Gravity Theories in More Than Four-Dimensions*, *Phys. Rept.* **137** (1986) 109.
- [21] X. O. Camanho, J. D. Edelstein, and A. Gomberoff, in progress.
- [22] R. Aros, R. Troncoso, and J. Zanelli, *Black holes with topologically nontrivial ads asymptotics*, *Phys.Rev. D* **63** (2001) 084015, [[hep-th/0011097](#)].
- [23] S. Carlip, *The Sum over topologies in three-dimensional Euclidean quantum gravity*, *Class. Quant. Grav.* **10** (1993) 207–218, [[hep-th/9206103](#)].
- [24] R. Zegers, *Birkhoff’s theorem in lovelock gravity*, *J.Math.Phys.* **46:072502,2005** (J.Math.Phys.46:072502,2005) 072502, [[gr-qc/0505016](#)].
- [25] C. Charmousis and J.-F. Dufaux, *General Gauss-Bonnet brane cosmology*, *Class. Quant. Grav.* **19** (2002) 4671–4682, [[hep-th/0202107](#)].
- [26] D. G. Boulware and S. Deser, *String Generated Gravity Models*, *Phys. Rev. Lett.* **55** (1985) 2656.
- [27] J. T. Wheeler, *Symmetric Solutions to the Gauss-Bonnet Extended Einstein Equations*, *Nucl. Phys.* **B268** (1986) 737.
- [28] J. T. Wheeler, *Symmetric solutions to the maximally Gauss-Bonnet extended Einstein equations*, *Nucl. Phys.* **B273** (1986) 732.
- [29] R.-G. Cai and K.-S. Soh, *Topological black holes in the dimensionally continued gravity*, *Phys. Rev.* **D59** (1999) 044013, [[gr-qc/9808067](#)].
- [30] R. B. Mann, *Black holes of negative mass*, *Class. Quant. Grav.* **14** (1997) 2927–2930, [[gr-qc/9705007](#)].
- [31] D. Kastor, S. Ray, and J. Traschen, *Smarr formula and an extended first law for lovelock gravity*, [arXiv:1005.5053](#).
- [32] G. T. Horowitz and R. C. Myers, *The AdS/CFT Correspondence and a New Positive Energy Conjecture for General Relativity*, *Phys. Rev.* **D59** (1998) 026005, [[hep-th/9808079](#)].
- [33] M. Marden, *Geometry of polynomials, Mathematical Surveys and Monographs* **3** (1949).

Providence, USA: Am. Math. Soc. (1949) 243 p.

- [34] C. Charmousis and A. Padilla, *The Instability of Vacua in Gauss-Bonnet Gravity*, *JHEP* **12** (2008) 038, [[arXiv:0807.2864](#)].
- [35] E. Witten, *Anti-de Sitter space and holography*, *Adv. Theor. Math. Phys.* **2** (1998) 253–291, [[hep-th/9802150](#)].
- [36] E. Witten, *Anti-de Sitter space, thermal phase transition, and confinement in gauge theories*, *Adv. Theor. Math. Phys.* **2** (1998) 505–532, [[hep-th/9803131](#)].
- [37] S. Nojiri and S. D. Odintsov, *Anti-de Sitter black hole thermodynamics in higher derivative gravity and new confining-deconfining phases in dual CFT*, *Phys. Lett.* **B521** (2001) 87–95, [[hep-th/0109122](#)].
- [38] Y. M. Cho and I. P. Neupane, *Anti-de Sitter black holes, thermal phase transition and holography in higher curvature gravity*, *Phys. Rev.* **D66** (2002) 024044, [[hep-th/0202140](#)].
- [39] R. C. Myers and J. Z. Simon, *Black Hole Thermodynamics in Lovelock Gravity*, *Phys. Rev.* **D38** (1988) 2434–2444.
- [40] S. Nojiri and S. D. Odintsov, *The de Sitter/anti-de Sitter black holes phase transition?*, [[gr-qc/0112066](#)].
- [41] M. Cvetič, S. Nojiri, and S. D. Odintsov, *Black hole thermodynamics and negative entropy in de Sitter and anti-de Sitter Einstein-Gauss-Bonnet gravity*, *Nucl. Phys.* **B628** (2002) 295–330, [[hep-th/0112045](#)].
- [42] I. P. Neupane and N. Dadhich, *Entropy bound and causality violation in higher curvature gravity*, *Class. Quant. Grav.* **26** (2009) 015013.
- [43] I. P. Neupane, *Black Holes, Entropy Bound and Causality Violation*, *Int. J. Mod. Phys.* **A24** (2009) 3584–3591, [[arXiv:0904.4805](#)].
- [44] R. Emparan, C. V. Johnson, and R. C. Myers, *Surface terms as counterterms in the AdS/CFT correspondence*, *Phys. Rev.* **D60** (1999) 104001, [[hep-th/9903238](#)].
- [45] T. Jacobson and R. C. Myers, *Black hole entropy and higher curvature interactions*, *Phys. Rev. Lett.* **70** (1993) 3684–3687, [[hep-th/9305016](#)].
- [46] I. P. Neupane, *Thermodynamic and gravitational instability on hyperbolic spaces*, *Phys. Rev.* **D69** (2004) 084011, [[hep-th/0302132](#)].
- [47] G. W. Gibbons and S. W. Hawking, *Cosmological event horizons, thermodynamics, and particle creation*, *Phys. Rev.* **D15** (1977) 2738–2751.
- [48] L. Vanzo, *Black holes with unusual topology*, *Phys. Rev. D* **D56** (1997) 6475–6483.
- [49] D. Birmingham, *Topological black holes in anti-de Sitter space*, *Class. Quant. Grav.* **16** (1999) 1197–1205, [[hep-th/9808032](#)].
- [50] P. H. Ginsparg and M. J. Perry, *Semiclassical Perdurance of de Sitter Space*, *Nucl. Phys.* **B222** (1983) 245.
- [51] T. Torii and H. Maeda, *Spacetime structure of static solutions in Gauss-Bonnet gravity: Neutral case*, *Phys. Rev.* **D71** (2005) 124002, [[hep-th/0504127](#)].
- [52] T. Torii and H. Maeda, *Spacetime structure of static solutions in Gauss-Bonnet gravity: Charged case*, *Phys. Rev.* **D72** (2005) 064007, [[hep-th/0504141](#)].
- [53] R. A. Matzner, N. Zamorano, and V. D. Sandberg, *Instability of the Cauchy horizon of*

- Reissner-Nordstrom black holes*, *Phys. Rev.* **D19** (1979) 2821–2826.
- [54] E. Poisson and W. Israel, *Internal structure of black holes*, *Phys. Rev.* **D41** (1990) 1796–1809.
- [55] P. R. Brady and J. D. Smith, *Black hole singularities: A Numerical approach*, *Phys. Rev. Lett.* **75** (1995) 1256–1259, [[gr-qc/9506067](#)].
- [56] M. Dafermos, *The interior of charged black holes and the problem of uniqueness in general relativity*, [[gr-qc/0307013](#)].
- [57] T. Torii, *Black holes in higher curvature theory and third law of thermodynamics*, *J. Phys. Conf. Ser.* **31** (2006) 175–176.
- [58] P. R. Anderson, W. A. Hiscock, and D. J. Loranz, *Semiclassical stability of the extreme Reissner-Nordstrom black hole*, *Phys. Rev. Lett.* **74** (1995) 4365–4368, [[gr-qc/9504019](#)].
- [59] D. Marolf, *The dangers of extremes*, *Gen. Rel. Grav.* **42** (2010) 2337–2343, [[arXiv:1005.2999](#)].
- [60] G. Dotti and R. J. Gleiser, *Linear stability of Einstein-gauss-bonnet static spacetimes. part. I: Tensor perturbations*, *Phys. Rev.* **D72** (2005) 044018, [[gr-qc/0503117](#)].
- [61] R. J. Gleiser and G. Dotti, *Linear stability of Einstein-Gauss-Bonnet static spacetimes. II: Vector and scalar perturbations*, *Phys. Rev.* **D72** (2005) 124002, [[gr-qc/0510069](#)].
- [62] M. Beroiz, G. Dotti, and R. J. Gleiser, *Gravitational instability of static spherically symmetric Einstein-Gauss-Bonnet black holes in five and six dimensions*, *Phys. Rev.* **D76** (2007) 024012, [[hep-th/0703074](#)].
- [63] T. Takahashi and J. Soda, *Stability of Lovelock Black Holes under Tensor Perturbations*, *Phys. Rev.* **D79** (2009) 104025, [[arXiv:0902.2921](#)].
- [64] T. Takahashi and J. Soda, *Instability of Small Lovelock Black Holes in Even- dimensions*, *Phys. Rev.* **D80** (2009) 104021, [[arXiv:0907.0556](#)].
- [65] T. Takahashi and J. Soda, *Catastrophic Instability of Small Lovelock Black Holes*, *Prog. Theor. Phys.* **124** (2010) 711–729, [[arXiv:1008.1618](#)].
- [66] T. Takahashi and J. Soda, *Master Equations for Gravitational Perturbations of Static Lovelock Black Holes in Higher Dimensions*, *Prog. Theor. Phys.* **124** (2010) 911–924, [[arXiv:1008.1385](#)].
- [67] X. O. Camanho, J. D. Edelstein, and M. F. Paulos, *Lovelock theories, holography and the fate of the viscosity bound*, [[arXiv:1010.1682](#)].
- [68] J. Crisostomo, R. Troncoso, and J. Zanelli, *Black hole scan*, *Phys. Rev.* **D62** (2000) 084013, [[hep-th/0003271](#)].
- [69] S. W. Hawking, G. T. Horowitz, and S. F. Ross, *Entropy, Area, and black hole pairs*, *Phys. Rev.* **D51** (1995) 4302–4314, [[gr-qc/9409013](#)].
- [70] E. Gravanis, *Shock waves and Birkhoff’s theorem in Lovelock gravity*, *Phys. Rev.* **D82** (2010) 104024, [[arXiv:1008.3583](#)].
- [71] S. Deser, R. Jackiw, and S. Templeton, *Three-Dimensional Massive Gauge Theories*, *Phys. Rev. Lett.* **48** (1982) 975–978.
- [72] J. Oliva and S. Ray, *A new cubic theory of gravity in five dimensions: Black hole, Birkhoff’s theorem and C-function*, *Class. Quant. Grav.* **27** (2010) 225002, [[arXiv:1003.4773](#)].
- [73] J. Oliva and S. Ray, *Classification of Six Derivative Lagrangians of Gravity and Static*

*Spherically Symmetric Solutions*, *Phys. Rev.* **D82** (2010) 124030, [[arXiv:1004.0737](#)].

[74] R. C. Myers and B. Robinson, *Black Holes in Quasi-topological Gravity*, *JHEP* **08** (2010) 067, [[arXiv:1003.5357](#)].

[75] R. C. Myers, M. F. Paulos, and A. Sinha, *Holographic studies of quasi-topological gravity*, *JHEP* **08** (2010) 035, [[arXiv:1004.2055](#)].